GENESIS OF TOURMALINIZATION IN DUTSEN DANBAKOSHI AREA, SHEET 56 (MUSAWA S.E) N.W NIGERIA

BY

Jamilu Garba GEZAWA, B.TECH. GEOLOGY (YOLA) 1997

M.Sc./Scie/02399/2009-10

A THESIS SUBMITTED TO THE SCHOOL OF POSTGRADUATE STUDIES, AHMADU BELLO UNIVERSITY ZARIA,

IN PARTIAL FULFILLMENT OF THE REQUIREMENTS FOR THE AWARD

OF A

THE DEGREE OF MASTER OF SCIENCE IN GEOLOGY

DEPARTMENT OF GEOLOGY,

FACULTY OF SCIENCE

AHMADU BELLO UNIVERSITY, ZARIA

NIGERIA

MARCH, 2013

DECLARATION

I declare that the work in this Project Report/ Thesis/Dissertation entitled ‘‘Genesis of Tourmalinization in Dutsen Danbakoshi Area, sheet 56 (Musawa S.E) N.W Nigeria’’ has been carried out by me in the Department of Geology Ahmadu Bello University, Zaria. Information derived from the literature has been duly acknowledged in the text and a list of references provided. No part of this project report/ thesis/dissertation was previously presented for another degree or diploma at this or any other institution

| --- | --- | --- |
| Name of Student | Signature | Date |

CERTIFICATION

The project report/ thesis/dissertation entitled GENESIS OF TOURMALINIZATION IN DUTSEN DANBAKOSHI AREA, SHEET 56 (MUSAWA S.E) N.W NIGERIA by JAMILU GARBA GEZAWA meets the regulations governing the award of the degree of Master of Science in Geology of the Ahmadu Bello University, and is approved for its contribution to knowledge and literary presentation

---	---	---
Name	Signature	Date
---	---	---
Chairman Supervisory Committee	Signature	Date
Dr. A. A. Ibrahim		
---	---	---
Member, Supervisory Committee	Signature	Date
Dr. T. Najime		
---	---	---
Head of Department Geology	Signature	Date
Prof. U. A. Danbatta		
---	---	---
Dean School of Postgraduate	Signature	Date
Prof. Joshua Adebayo		

ACKNOWLEDGEMENTS

All thanks belong to Allah (S.W.T) the Beneficent, the Merciful, the Sustainer, the Self Subsistent and the Eternal; by His grace this work was accomplished. I wish to acknowledge with profound gratitude the guidance of Prof. E. C. Ike throughout the period of this work. He always treated this work with high degree of professionalism and competence. I also acknowledge Dr. A. A. Ibrahim for his patience in going through this work and always making good comments which further helped in refining this work. I wish to thank Dr. T. Najime for making valuable contributions toward the successful completion of this work.

I thank my mother, Hajiya Fatima Muhammad, for her encouragement and consistent prayers for the success of this work. I am also grateful to my mentor Prof. Ibrahim Garba, who was always ready to assist at any time. My profound gratitude extends to my religious guidance Hujjatul Islam Hamzah Muhammad Lawal. His advice and assistance will always be remembered.

I am highly indebted and grateful to the Chairman, Freedom Radio F.M, Air Vice Marshall Muktar Muhammad and some members of the Board of Directors especially Alhaji Ado Muhammad, Alhaji Bello Maisudan and Alhaji Aminu Dalhatu. Their assistance and encouragement will never be forgotten. I am deeply touched by the assistance and help rendered by Engineer Muktar Ibrahim Bature. He was always ready to help whenever needed.

Special gratitude goes to Prof Robert F. Martin of Mc Gill University, Montreal, Canada and Malam Shehu Magaji Suleiman of Department of Geology Ahmadu Bello University Zaria. Their assistance is highly appreciated.

I wish to send special thanks to the following people: Alhaji Sanusi Ado Bayero (Chiroman Kano), Alhaji Uba Leader, Shafiu Ahmad Rufai, Hajiya Saratu Dalhatu, Dr Lawan Garba, Prof Umar Adamu Danbatta, Salihi Abubakar Dawaki, Aminu Salihi Ahmad, Abdulaziz Murtala Ahmad, Lawan Bello Ahmad, Alhaji Muhammad Sulley, Dr Garba Ibrahim Bichi, Abubakar Abdullahi Beli, Mr Festus Ikenna, Wing Com Hadi Shehu Ahmad, Sulaiman Ado Muhammad, Prof U. A. Lar, Alh. Ma'amun Da'u Aliyu for their contribution to this work, may Allah reward them accordingly.

Finally, I wish to thank all those people that have assisted in one way or another but their names are not mentioned.

DEDICATION

To Imam Mahdi (A.S) the Awaited Saviour. May Allah (S.W.T) hasten his reappearance. Ameen.

ABSTRACT

Field mapping in Dutsen Danbakoshi was carried out using topographical map of Musawa SE sheet 56 on a scale 1: 50, 000 and the quartz-tourmaline ridges were further mapped on a scale of 1: 10, 000 to study it in a more detail. Petrographic studies were conducted using both transmitted and reflected light microscope. The geochemical analysis of 21 representative samples was carried out using X-ray fluorescence, inductively coupled sector field mass spectrometry and mass spectrometry.

Field mapping reveals that the area is underlain by Older Granite, Metasandstone, and Diorite as the major rock types. Quartz-tourmaline ridges occur as minor intrusive. These rocks have been deformed; sheared with the joints trending N-S to NNE-SSW, which coincided with the pattern of the Pan-African basement structures.

Petrographic studies have shown that the granites are composed of quartz, microcline and biotite as major minerals; the Diorite is composed of plagioclase, hornblende, quartz and biotite. The Metasandstone consists mainly of quartz and feldspar. The quartz–tourmaline is principally composed of tourmaline and quartz.

Geochemical and isotopic analyses results show that SiO_2 in granites to be 72.71-67.30 wt%, diorite 48.38-38.90 wt% and quartz-tourmaline 57.97-35.41 wt% while K_2O in granite 6.98-4.43 wt%; diorite 1.08-0.02 wt% and quartz-tourmaline 0.01-0.19 wt%. The trace element composition shows enrichment of Sr (1200-0.036 ppm), Rb (319-0.038 ppm), Ba (1000-0.04 ppm). The rare earth elements in the samples show enrichment in La (87.9-12 ppm), Nd (64.1-9.5 ppm), Ce (163-0.11 ppm), Eu (1.66-0.13 ppm), Tb (1.5-0.3 ppm), Ho (1.6-0.3 ppm), Lu (0.68-0.11 ppm), and boron isotope ($\sigma\ ^{11}B$) in the quartz-tourmaline ranges from -15.84‰ - 17.92‰

Various discrimination diagrams were used to classify the rock types and their tectonic settings. The granites plot in syncollisional field. Based on REE distribution pattern and their enrichment of LREE and depletion of HREE, they are of continental or crustal origin. The negative Eu anomaly is probably indicating the formation of both the host rocks (granite and diorite) and quartz-tourmaline in Upper Proterozoic metasedimentary environment. The negative Ce anomaly is signifying the formation of quartz-tourmaline under oxidizing conditions.

The host rocks (granite and diorite) and quartz-tourmaline are both enriched in LREE and depleted in HREE with negative Eu anomaly indicating syngenetic relationship.

Boron isotope values ($\sigma\ ^{11}B$) of quartz-tourmaline ranges from (– 15.84‰ to – 17.92‰) thus signifying continental or crustal origin of the boron enriched residual fluids which led to the tourmalinization and also indicating possible dual provenance of tourmaline to be high pressure metamorphic rocks or granite and pegmatite. The boron isotope values also suggest that the granitoids from which the B enrich residual fluids were generated were probably originated as a result of the reworking of preexisting basement complex rocks.

TABLE OF CONTENTS

Title page	i
Declaration	ii
Certification	iii
Acknowledgements	iv
Dedication	v
Abstract	vi
Table of content	viii
List of Figures	xii
List of Tables	xiii
List of Plates	xiv
List of Appendices	xvi

Chapter 1 **GENERAL INTRODUCTION**

1.1	Background of the Study	1
1.2	Location and Accessibility	2
1.3	Climate and Vegetation	4
1.4	Relief and Drainage	4
1.5	Previous Works	4

1.6 Objectives and Scope of the Present work 7

Chapter 2 **REGIONAL GEOLOGY AND TECTONICS**

2.1 Introduction 8

2.2 Gneisses and Migmatites 8

2.3 Schist Belts 9

2.3 Older Granites 11

2.4 Tectonic evolution of the Nigerian basement complex 13

Chapter 3 **FIELD GEOLOGY AND PETROGRAPHY**

3.1 Preamble 14

3.2 Granite 14

3.3 Diorite 20

3.4 Quartz-tourmaline 23

3.5 Quartzite rock 30

3.6 Metasandstone 32

Chapter 4 **STRUCTURAL GEOLOGY**

4.1 Preamble 34

4.2 Shears 34

4.3 Joints 35

Chapter 5 **GEOCHEMISTRY**

5.1 Sample collection and analytical techniques 40

5.2 Geochemical analysis result 44

5.3 Geochemistry of Granite 48

5.3.1 Major elements distribution 48

5.3.2 Trace elements distribution 48

5.4. Geochemistry of Diorite 50

5.4.1 Major element distribution 50

5.4.2 Trace elements distribution 50

5.5 Geochemistry of the Quartz-tourmaline 52

5.5.1 Major element distribution 52

5.5.2 Trace elements distribution 52

5.5.3 Boron isotope 53

5.6 Discussions 54

5.7 Mode of origin 60

Chapter 6 **CONCLUSION AND RECOMMENDATION**

6.1 Conclusion 61

6.2 Recommendation 62

References 63

Appendices 73

LIST OF FIGURES

Fig 1.0 Geological map of Nigeria showing the study area 3

Fig 2.0 Regional geology of the Pan-African belt 10

Fig 2.1 Geological map of Nigeria showing the schist belts 12

Fig. 4.0 Rose diagram of joint trends in medium grained granite 37

Fig. 4.1 Rose diagram of joint trends in medium grained granite 39

Fig. 5.0 Chondrite-normalized REE patterns for granitic rocks of Dutsen Danbakoshi 49

Fig.5.1 Chondrite-normalized REE patterns of diorite rock of the study area 51

Fig. 5.2 Chondrite-normalized REE patterns for the quartz-tourmaline of the study area 53

Fig. 5.3 Discrimination diagram of the granite from the study area 54

Fig. 5.4 Chondrite-normalized REE patterns for the rocks of Dutsen Danbakoshi area with granite = black, diorite = green and quartz tourmaline = blue. 56

Fig. 5.5 Compilation of boron isotope data of tourmaline from different host-rock and various inferred sources of boron. 59

Fig. 6 Geological map of the study area (in pocket)

LIST OF TABLES

Table 1 Major element concentrations of the rocks in study area 45

Table 2 Trace element concentrations of the rocks in study area 46

Table 3 Rare earth element concentrations of the rocks in study area 47

Table 4 Boron isotope values of the quartz-tourmaline 47

Table 5 Chondrite-normalized REE values of granite 49

Table 6 Chondrite-normalized REE values of diorite 50

Table 7 Chondrite-normalized REE values of quartz-tourmaline 53

LIST OF PLATES

Plate 1	Photograph of fine grained granite at Garkuwa	15
Plate 2	Photomicrograph of fine grained granite showing various minerals ppl x 15	16
Plate 3	Photomicrograph of fine grained granite showing various minerals xpl x 20	17
Plate 4	Photograph of medium grained granite showing its boulder nature	18
Plate 5	Photomicrograph of medium grained granite showing minerals ppl x 25	19
Plate 6	Photomicrograph of medium grained granite showing various minerals xpl x 25	19
Plate 7	Photograph of diorite boulders near Shanono	20
Plate 8	Photomicrograph of diorite showing various distribution of minerals ppl x 10	21
Plate 9	Photomicrograph of diorite showing various distribution of minerals xpl x 20	22
Plate 10	Photograph of quartz-tourmaline rock in massive form and highly fractured	23
Plate 11	Photomicrograph of quartz-tourmaline showing tourmaline, biotite ppl x 15	24
Plate 12	Photomicrograph of quartz-tourmaline showing tourmaline, quartz xpl x10	24
Plate 13	Photomicrograph of quartz-tourmaline showing tourmaline, biotite ppl. x 10	25
Plate 14	Photomicrograph of quartz-tourmaline showing tourmaline, quartz ppl x20	26
Plate 15	Photomicrograph of quartz-tourmaline showing tourmaline, quartz xpl x20	26
Plate 16	Photomicrograph of quartz-tourmaline showing tourmaline, quartz ppl x15	27
Plate 17	Photomicrograph of quartz-tourmaline showing tourmaline, quartz xpl x15	27
Plate 18	Photomicrograph of quartz-tourmaline showing tourmaline, quartz	28
Plate 19	Photomicrograph of quartz-tourmaline showing tourmaline, quartz	29
Plate 20	Photograph of quartzite in massive form and highly fractured	30
Plate 21	Photomicrograph of quartzite showing tourmaline and quartz ppl x 15	31
Plate 22	Photomicrograph of quartzite showing tourmaline and quartz xpl x 20	31
Plate 23	Photograph of Metasandstone showing the effect of weathering	32

Plate 24 Photomicrograph of Metasandstone showing various quartz crystals ppl x 10 33

Plate 25 Photomicrograph of Metasandstone showing quartz and feldspar xpl x 10 33

Plate 26 Photograph showing fracture along quartz-tourmaline ridge 35

Plate 27 Showing geometry of joints as observed in medium grained granite 36

Plate 28 Showing geometry of joints as observed in the medium grained granite 38

APPENDIXES

Appendix 1 Joint readings (in degrees) on the medium grained granite 73

Appendix 2 Joint readings (in degrees) on the medium grained granite 74

CHAPTER 1

GENERAL INTRODUCTION

1.1 Background of the Study

The study area lies within Malumfashi schist belt that is underlain mainly by muscovite and muscovite-biotite schists and phyllites interbedded with thin quartzite units (McCurry, 1973). The pelitic rocks include minor graphitic and feldspathic schists, and contain frequent quartz and quartz-tourmaline veins. Interbedded quartzite units are generally thin but may be grouped to give sections which are dominantly quartzite and units of well bedded quartzite, several tens of meters thick. Minor rocks such as spessartite quartzite, calc-silicate rocks and anthophyllite cordierite schist also occurs. Amphibolites also form occasional discontinuous bands (Turner, 1983).

Tourmaline is a boron silicate mineral compounded with elements such as Aluminium, Iron, Magnesium, Lithium or Potassium. Tourmaline is classified as a semi-precious stones and the gem comes in a wide variety of colours .The general chemical formula may be written as: $X\ Y_3\ Z_6\ (T_6\ O_{18})\ (B\ O_3)\ V_3\ W$, where,

X = Ca, Na, K

Y = Li, Al, $Fe^{2+,}$ Mn^{2+}, Zn, Mg, Cr^{3+}, Fe^{3+}, Ti^{3+}

Z = Mg, Al, Fe^{3+}, Cr^{3+}, V^{3+}

T = Si, Al, B

B = B

V = OH, O

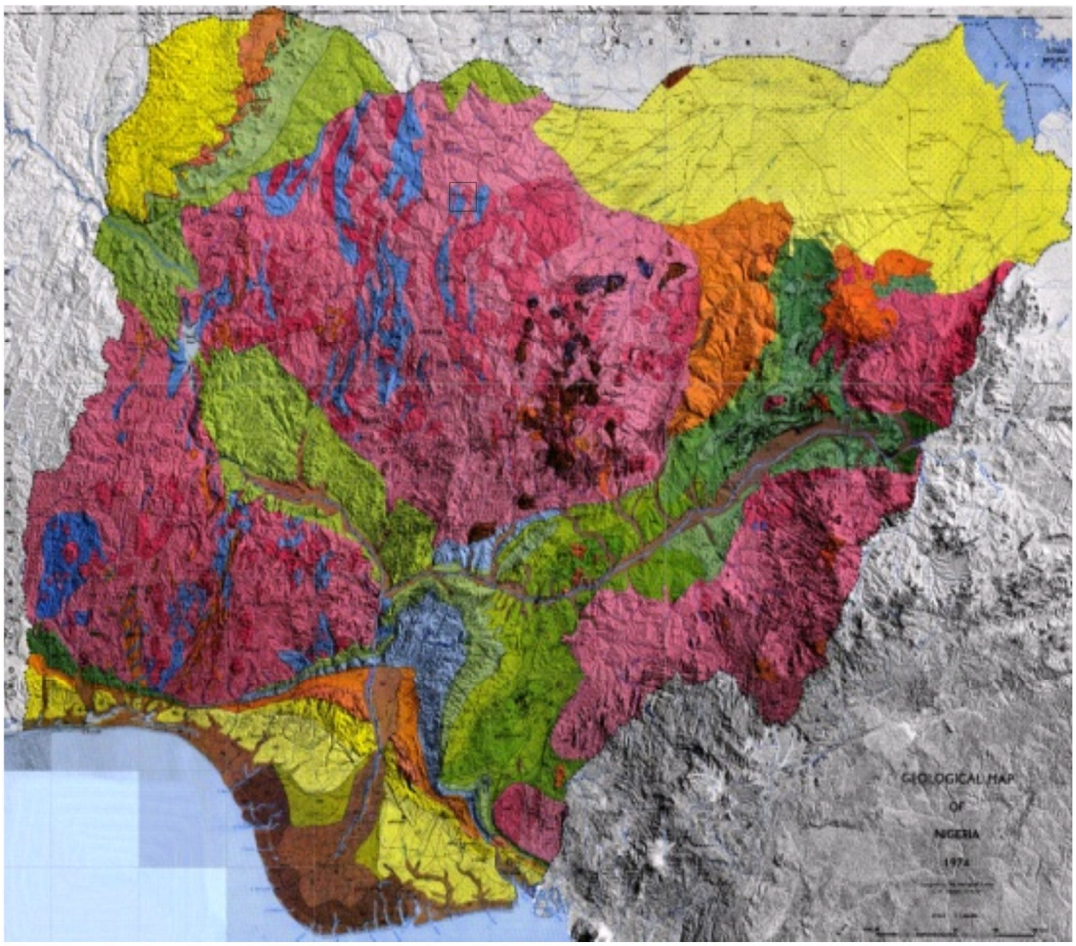
W = OH, F, O

Prior to this study, only few published works on tourmalinization most especially in Malumfashi schist belt are available, this situation coupled with availability of modern geochemical analytical methods argues for the need to study tourmaline rich rocks in Dutsen Danbakoshi in order to determine the origin or source of the fluids that precipitated them.

1.2 Location and Accessibility

The study area lies between latitude 12º 00’ 00’’ to 12º 05’ 00’’ N and longitude 7º 55’ 00’’ to 8º 00’ 00’’ E and. It constitutes part of Musawa Sheet 56 S.E and lies within Shanono Local Government Area of Kano State.

The area is fairly accessible from various motorable roads, foot paths, cattle tracks and numerous river channels. The Gwarzo – Shanono tarred road traverse the eastern portion of the study area. An untarred but motorable road from Dalanba – Danbakoshi – Gasawa traverses through the western part of the area



Migmatite/Gneiss and Older Granites

Metasedimentary rocks

Younger Granites

Study area

Older basalts/Tertiary basalts

Sandstone/conglomerates, silt

Clays, Shales and Limestones

Fig. 1 Geological map of Nigeria showing N.E part of Malumfashi Schist and the study area, after Geological survey of Nigeria 1974

1.3 Climate and Vegetation

The study area falls within Tropical Continental Climatic Zone and is characterized by two distinct seasons. The rainy season begins from May and terminates in October, while the dry season commences in November terminating in April. The highest temperature is recorded between March and May while the lowest values are experienced from December to February during Harmattan.

The vegetation is typically Sudan Savannah and is characterized by thorny bush, trees, shrubs, and grasses.

1.4 Relief and Drainage

The area is generally undulating with the highest peak located at Dutsen Danbakoshi hill in the western portion of the area, while the lowest elevation occurs within the river Magaga channels.

The general relief of the area is defined by low lying ridges, isolated hills, inselbergs and minor domes sharply differentiated from less distinct topography of the surrounding areas. All the streams and tributaries of river Magaga in the area are seasonal, flowing only during rainy season. Drainage patterns are mostly dendritic.

1.5 Previous Work

Many works has been done on the Basement Complex of North Western Nigeria, most especially the Malumfashi schist belt. The earliest work was reported by Fargher (1961) on the geology of part of the crystalline basement of Northern Nigerian is that McCurry (1970), however mapped,

large areas such as Zaria, Sokoto, and western part of Katsina in N.W Nigeria, part of which is Musawa sheet 56, where she to identifies three groups of rocks namely:

(a) Migmatite-Gneiss, as the oldest

(b) Schist Belts

(c) Older Granites series of Pan African age which are the youngest.

There are thirteen schist belts in Nigeria, one of which is the Malumfashi schist belt which is located around the present study area.

Ajibade (1982) described the silicified fault zone in the gneissic complex of Malumfashi area and outlines the significance to the major rock types found in the area as indicating the presence of a fault. Two major dextral strike-slip NE-SW trending regional faults have been established in Nigeria. These are the Anka-Yauri-Isenyi (AYI) and the Kalangai-Zungeru-Ifewara (KZI) faults. Wright (1976), Ball (1980).

Garba (1996) showed that tourmaline content could be used in deciphering the physico-chemical conditions of gold mineralizing fluids in the Bin Yauri area. Shabaga et al., (2010) uses boron and lithium isotopic compositions to determine the origin of Cu-bearing tourmalines in Nigeria, Brazil and Mozambique.

There is no previous geologic report on the occurrence of quartz-tourmaline in Dutsen Danbakoshi. However, tourmaline and tourmaline rich rocks occurs in various geologic environments and settings such as metamorphic, igneous, sedimentary and metasedimentary. Although tourmaline constitute no more than a few percent of any rock type, tourmaline–rich

rocks are defined as tourmalinites or quartz-tourmaline having lithological unit broadly concordant with their enclosing host rocks and containing in excess 15–20 Vol % tourmaline; Nicholson (1980), Slack (1982); Slack et al., (1984); are documented in a variety of geologic settings particularly in metasomatised granites and metasedimentary sequences Ethier and Campbell (1977); Henry and Guidotti (1985); Slack and Coad (1989); Garba (1996); Slack et al., (1996). It occurs in metamorphic rocks having a wide range of bulk composition under various metamorphic grades Slack et al., (1984); Slack and Coad (1989); Henry and Dutrow (1992); Willner (1992).

The chemical variability of tourmaline can provide useful information on the physico chemical changes occurring during formation of its host rock (Manning, 1982); Henry and Guidotti (1985), Gallagher (1988). Being a chemically resistant mineral Werding and Schreyer (1984) it potentially preserves the chemical signatures of multiple hydrothermal and metamorphic event Slack and Coad (1989); Michialidis (1998).

In recent years due to large compositional range of tourmaline in term of both major and trace elements makes it a sensitive indicator of the composition of its host rocks. Tourmalines have been shown to capture signature of their host's bulk composition, including elevated Li where formed in pegmatite (Keller et al., 1999), Selway et al., (1999, 2000), Hezel et al., (2011), London (2011), and high Ni, V and Cr where present in metabasic rocks, metabauxites and metamorphosed anoxic sediments (Henry and Dutrow, 2001), Bacik et al., (2011). Distinct signatures related to transient episodes of hydrothermal fluid circulation have also been widely reported Keller et al., (1999), Williamson et al., (2000), and Trumbull et al., (2011). These signatures have been used in sedimentary provenance studies (Henry & Dutrow, 1996),

Nascimento et al., (2007), as well as in understanding of and exploration for ores (Dommanget et al., 1993, Kusnir, 1999, Deksissa and Koeberl, 2002), Baksheev et al. (2011), Trumbull et al. (2011). In roads are now being made in quantifying the element portioning in tourmaline and coexisting melt, fluid and minerals, using natural samples and laboratry experiments (Von Goerne and Franz, 2000, Von Goerne et al., 2001, Klemme et al., 2011, Van Hinsberg and Schumacher, 2011). This will eventually allow these qualitative chemical signatures to be converted into quantitative compositional monitor of the host environment.

1.6 Objectives and Scope of the Present work

The aim of this study is:

(1) To undertake geological mapping of Dutsen Danbakoshi and its environment with objectives of:

(a) Studying the lithology and field relationships of the constituent rock units in the area

(b) Redefining (where necessary) the geological boundaries of the various lithological units in the area

(2) To identify and describe the petrography, geochemistry and boron isotope composition of Quartz-tourmaline rocks with the objective of:

(a) Establishing the possible origin and source of the fluid that led to the tourmalinization

CHAPTER 2

REGIONAL GEOLOGY AND TECTONICS

2.1 Introduction

The Nigerian Basement Complex is a part of an Upper Proterozoic – Lower Phanerozoic Pan African (600 ± 150 Ma) mobile belt situated between the West African and the Congo Cratons (Garba, 2003b). The belt is made up of two sectors the Tuareg shield and the Togo – Benin Shield as shown in Fig 2.

The Nigerian Basement is part of the Pan-African mobile of Kennedy (1964) as all crystalline shield areas have been reworked (c. 600 Ma). Apart from the Jurassic ring complexes, most crystalline rocks of the Nigerian basement bear Pan-African tectonics and mineralogical imprints, Pre-Pan African ages in Nigeria are therefore protolith ages (Dada, 1998). Geochronological evidence indicates that the Nigerian basement is polycyclic and includes rocks of Archaean (2.0-3.0 Ga) era together with those of Eburnean (2000 ± 200 Ma) and Pan African (750-450 Ma) event (Turner, 1983; Fitches et. al., 1985; Ajibade et. al., 1987; Elueze, 2000). Rocks of the Nigerian basement complex are divided in to three units (Fitches et. al., 1985; Ajibade et. al., 1987); namely: Gneisses and Migmatites, Schist Belts and Older Granites

2.2 Gneisses and Migmatites

Gneisses and migmatites with entrained supracrustal relics.whose metamorphism is generally in the amphibolite facies grade. These rocks are mainly quartzites, amphibolites, calcareous rocks, biotite hornblende gneisses, quartz schist and biotite hornblende schist (Wright et al., 1985).

2.3 Schist Belts

The Nigerian schist belts occur in a 300 km wide zone, predominantly west of longitude 8^0 E, which trends NNE, parallel to the boundary between Pan African and the West African Craton (Turner, 1983; Fitches et.al., 1985; Ajibade et.al.,1987; Adekoya, 1996). The schist belt zone is flanked by migmatite-gneiss-granite terrain to the East and West, and the same terrain separates the individual belts within the zone(Turner, 1983; Ajibade et.al., 1987). The schist belts are metasedimentary-volcanic, deformed, low grade (green schist facies) rocks Turner (1983), Fitches et.al, (1985).

There are difficulties in establishing actual and relative ages of the Nigerian schist belt. They were assigned collectively to the subsurface stage of the Pan African Orogenic cycle by McCurry, (1973, 1976, 1978), Wright and McCurry (1970), Grant (1969) and Burke and Dewey (1972) among others. More interpretations, however have pointed to the possibility of more than one generation of schist Grant (1978) used structural and lithological criteria together with isotopic signatures to distinguishing an earlier Kibaran (c. 1100Ma) Kushaka schist belt from the Pan African (700 – 600 Ma) Birnin Gwari schist Belt in NW Nigeria. This view was supported by Turner (1983) who using similar criteria assigned all Nigerian schist belts to one or other cycle. This hypothesis appears to explain the c. 1100 Ma isotopic age obtained by Ogezi (1977) from phyllites of the Maru belt Holt et al., (1978) and the Kibaran isotopic over printing of basement gneisses in several regions Grant et al., (1972). It also corroborates Hubbard's (1975) interpretation of schist belt relations in south central Nigeria. The first obvious characteristic of the schist belt is ubiquitous presence of low to medium grade metasedimentary and metavolcanic rocks and their NNE-SSW trends. The schist belt occur predominantly as series of synformal

trough and strike ridges, intercalated with relic of migmatites and gneisses or intruded granite which separate and or lie within them.

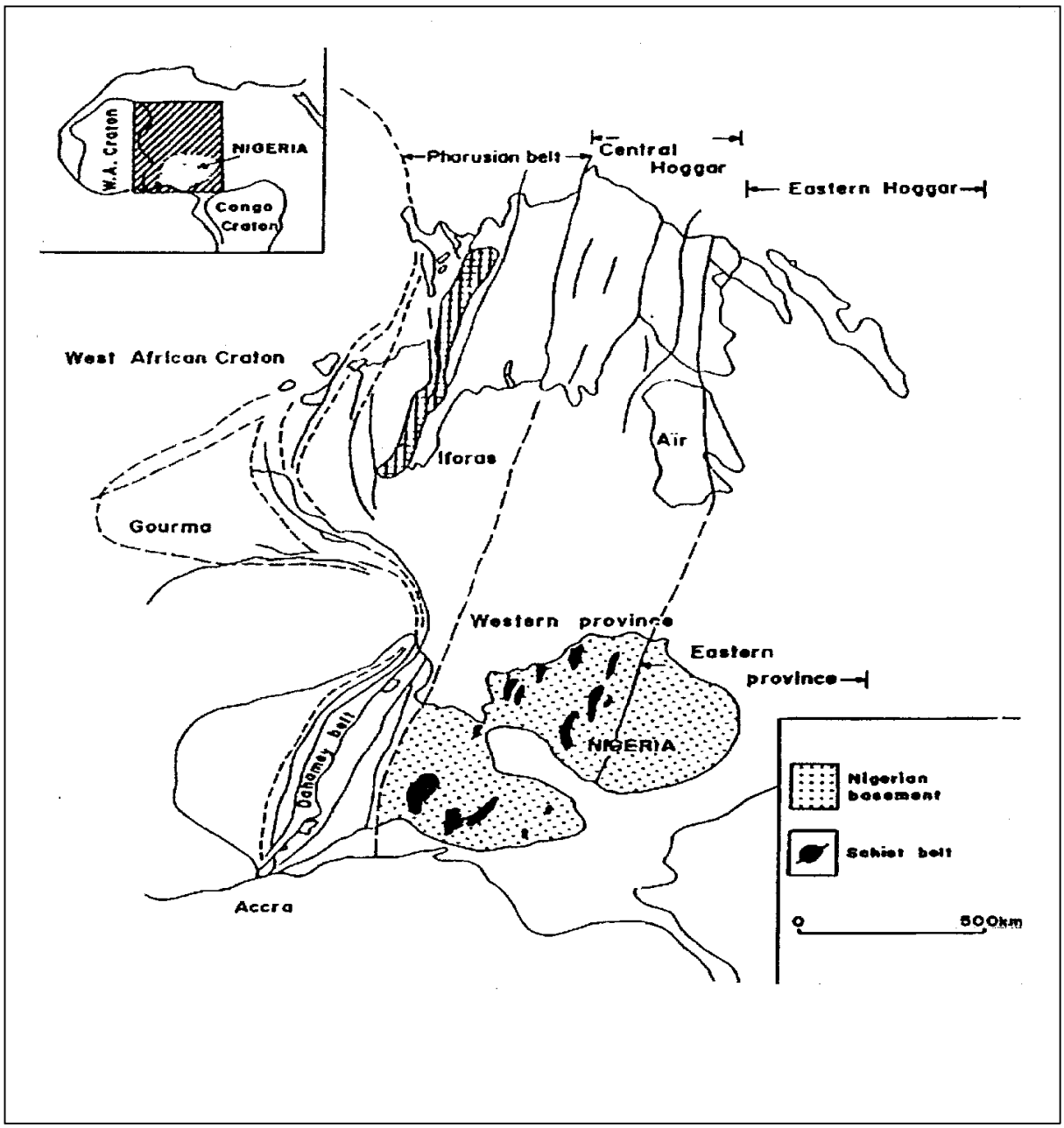


Fig 2 Geological map of the Pan-African belt East of the West African craton showing the relative positions of the Nigerian basement and the Tuareg shield. After Ajibade et al., (1987).

Wright and McCurry (1970) and Hubbard (1975) compared outcrop pattern of the schist belt to that of the Achaean Greenstone belt critical importance in comparing the two belts is their bulk composition. The schist belts have predominantly clastic sediments with minor volcanic rocks, this differentiates them from Greenstone belts elsewhere (e.g.) Ekwueme and Attoh (1997) which predominantly consist of volcanic rocks.

All the schist belts are predominantly composed of metamorphosed pelitic and semi-pelitic rocks Ekwueme (1995a) but each belt differs in the amount of such lithologies as conglomerates greywackes, quartzites, calcareous rock and volcanic rocks.

Turner (1983) and Ajibade et al., (1987) identified and classified thirteen main schist belts in the northwestern and northcentral Nigeria. These schist belts include the Birnin Gwari, Kushaka, Wonaka, Zuru, Anka, Maru Ushama, Malumfashi, Kazaure ,Ilesha, Igarra, Isenyi-Oyan belts as in Fig 2.1.

2.4 Older Granites

The Older Granites suites are considered as syntectonic to late tectonic granitoids emplaced during the Pan African orogeny. These granites intrude both the migmatite-gneiss complex and the schist belt. Earlier granitoids are foliated calc-alkaline granodiorite intrusions, while later undeformed late tectonic intrusions are monzonitic, sub alkaline to alkaline in character McCurry, (1989). Other rocks varieties constituting the older Granites suite include diorites, gabbros, charnockites and late tectonic high level volcanic and hypabysal rocks.

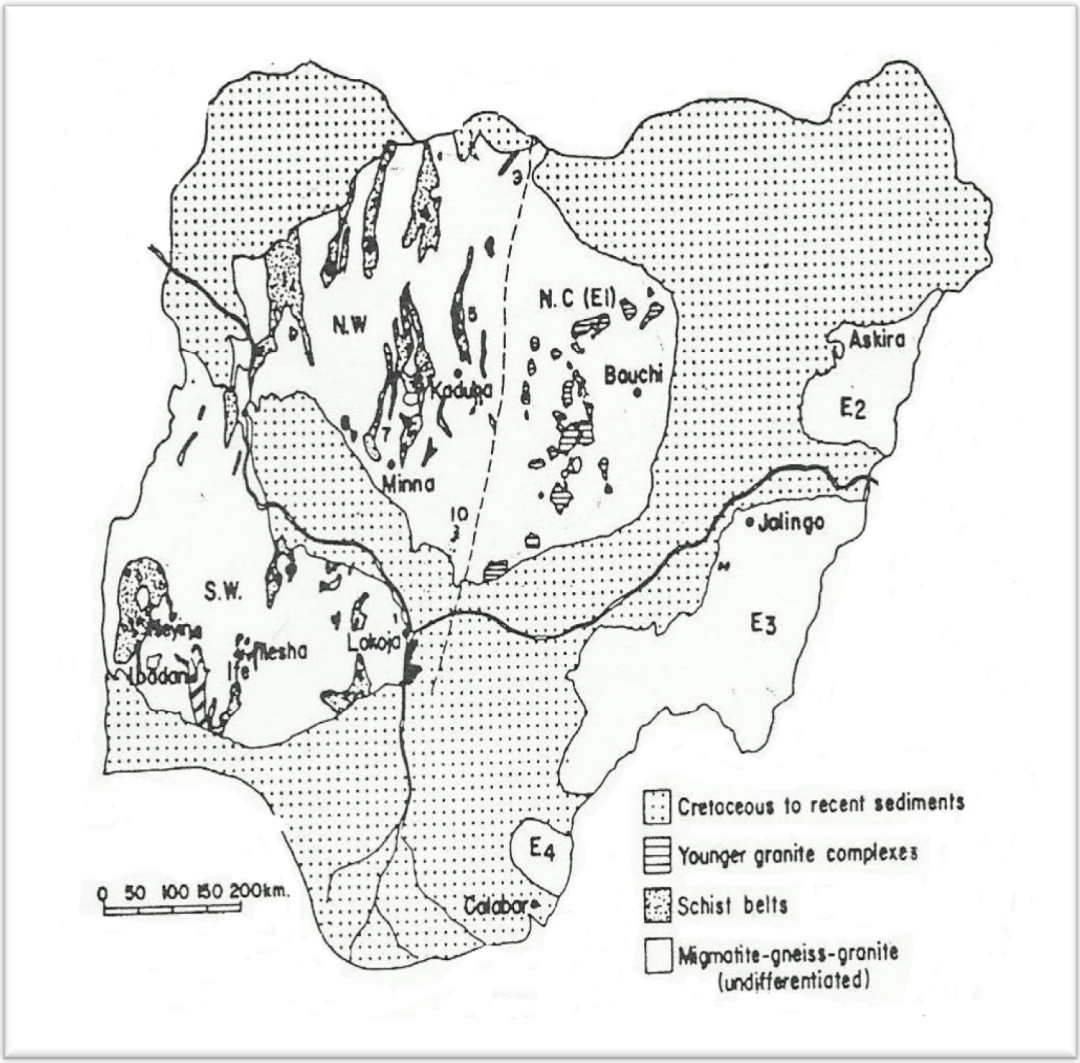


Fig 2.1 Simplified geological map of Nigeria. The schist belts are 1-Zuru, 2-Anka, 3-Maru, 4-Wonaka, 5-Malumfashi, 6-Kushaka, 7-Birnin Gwari, 8-Ushama, 9-Kazaure, 10-Toto belts, 11. Ilesha, 12 Igarra, 13 Isenyi-Oyan. After Ajibade et. al, 1987.

2.5 Tectonic Evolution of the Nigerian Basement Complex.

A collision type orogeny has been suggested by Turner (1983), Wright et al., (1985) involving the Pan-African shield and the West African Craton in which a subduction zone dipped east ward beneath the Pan African province Ajibade and Wright (1989). The Nigerian schist belts are thought to have been deposited in back-arc basins which developed after the onset of seduction at West African cratonic margin at about 1000 Ma. The closure of the ocean at the cratonic margin at about 600 Ma led to deformation, metamorphism and emplacement of the older Granites. The last manifestation of the Pan African event includes uplifts, acid volcanism and development of fault and shear zones.

There is however, increasing evidence that the Pan African collision involved more of an aggregation of crustal blocks rather than between the West African Craton and the Pan African Craton as a single entity. This is led Ajibade and Wright (1989) to propose that the Pan African collision was probably between mosaic Island arcs, sedimentary basins and continental fragments.

CHAPTER 3

FIELD GEOLOGY AND PETROGRAPHY

3.1 Preamble

The geologic field mapping was carried out using ground traverses provided by roads and footpaths, as well as river and stream courses. Topographical map on a scale of 1:50,000, Aeromagnetic map on a scale of 1:100,000 covering the whole project area and a GPS (Global Positioning System) instrument were used for the exercise.

The field work was started on 7 December 2009 and lasted for the period of two weeks. However further visit to the area were made to cross check certain observation. During the mapping exercise emphasis was laid on exact location of rock types and the boundaries.

The Quartz-tourmaline ridges were studied in greater detail on the scale of 1:10,000 and representative sample were collected systematically

The lithological units mapped in the study area include Granite, Metasandstone, Diorite, and Quartz-tourmaline.

Fifteen (15) thin sections were produced from representative rock samples from study area and were studied using reflected and transmitted light microscopes.

3.2 GRANITE

Granite occurs in both western and eastern parts of the study area at Dalanba, Garkuwa, Shanono, Danbakoshi and Gasawa, and can be texturally grouped into fine and medium grained. They constitute about 80% of the study area as in Fig 6.

3.2.1 Fine grained Granites

The fined grained Granite constitute about 20% of the study area and outcrops as well exposed ridges and inselbergs, they are mostly found in the eastern part of the area from Dalanba, Garkuwa and shanono, and occupies the lowest elevation in the study areas.



Plate 1 Outcrop of fine grained granite at Garkuwa village (Loc 3 E 12^0 03' 12'' E 7^0 56' 13'')

The fine grained Granite under the microscope is unfoliated equigranular rock composed of quartz, feldspars, biotite, and muscovite (Plate 2) Quartz constitutes 40% (visual estimation) and appears white to yellowish. Microcline is the dominant feldspar and occurs as subhedral crystal in places with inclusions of muscovite and quartz. Plagioclase feldspars are also present mostly as small crystal; feldpars constitute about 35% of the specimen.

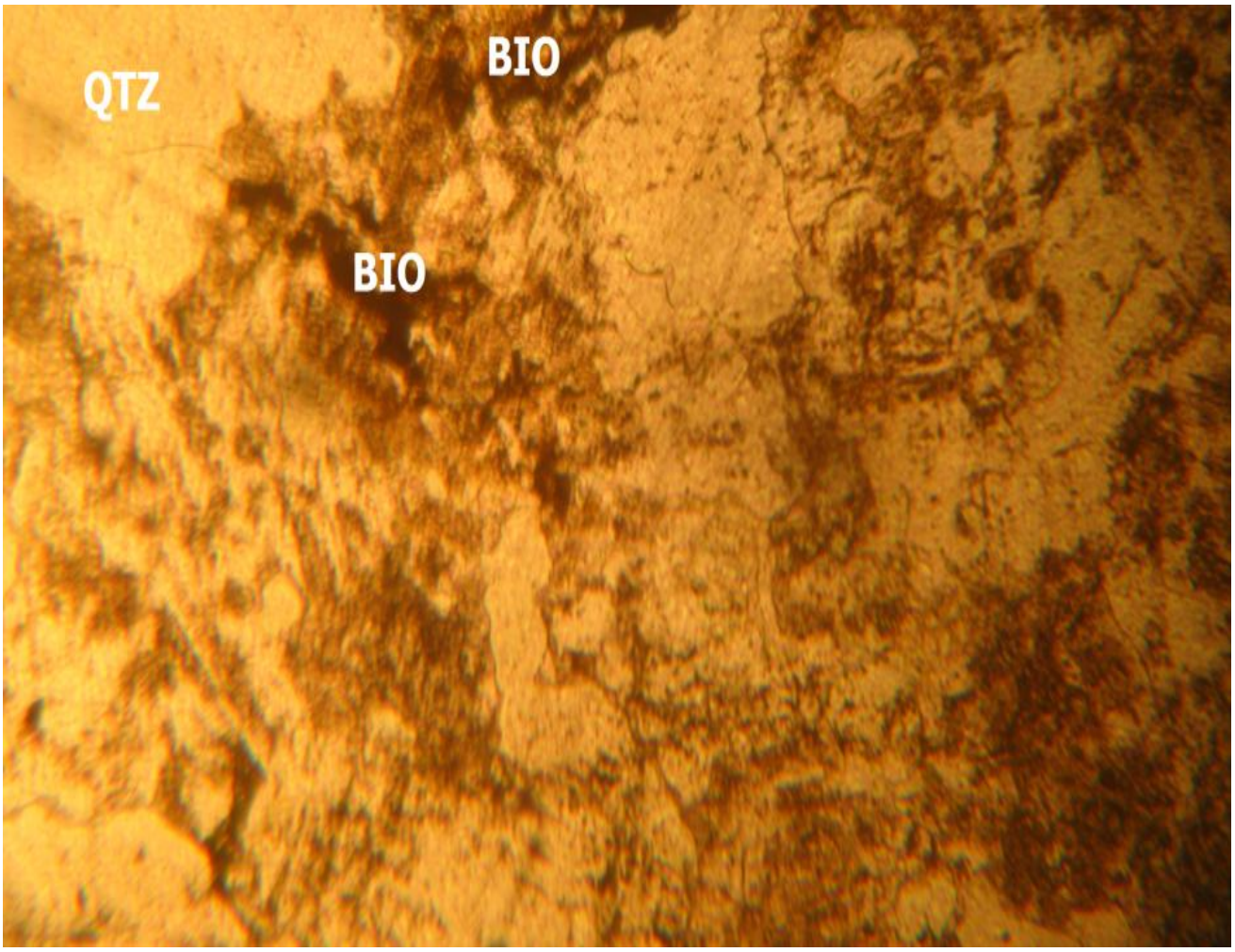


Plate 2 Photomicrograph of granite Sample no 3 showing subhedral biotite (BIO), and enhedral quartz (QTZ), ppl x 15.

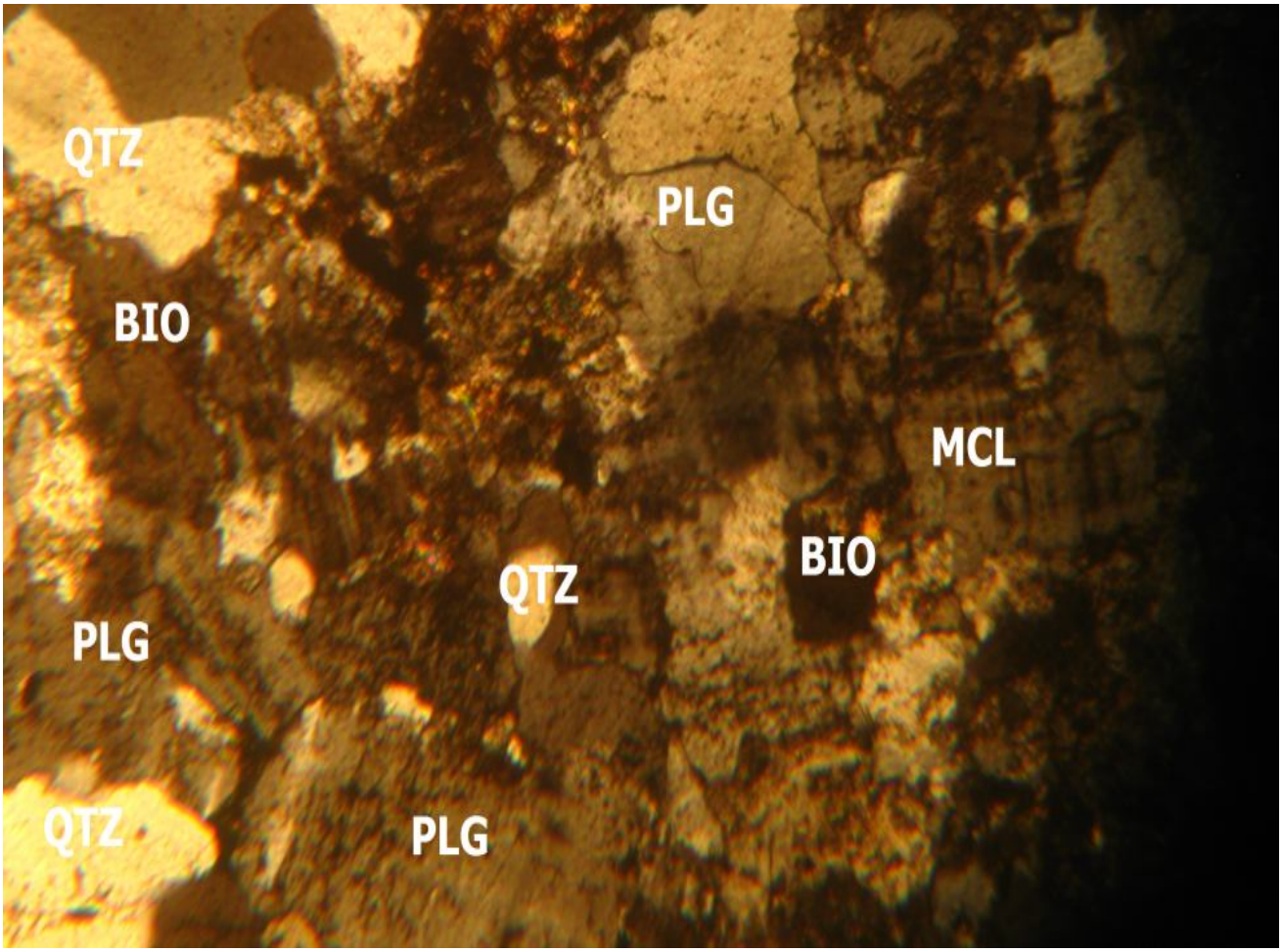


Plate 3 Photomicrograph of granite . Sample no 3 showing subhedral biotite (BIO) and enhedral quartz (QTZ), plagioclase feldspar (PLG) and microcline (MCL), xpl x 20

The dominant mica in the granite is biotite which occurs as thin crystals distributed throughout the body of the rock. Muscovite occurs also as flakes of various sizes with characteristic pleochroism and intermediate to high birefringence colour.

3.2.2 Medium grained Granites

The medium grained Granite constitutes about 60% of the study area. It is exposed as domes and inselbergs such as those shown in Plate 4. They are mostly confined to western part of the study area from Gasawa to DanBakoshi and beyond.



Plate 4 Medium grained granite showing its fractured and bouldery nature at Gasawa (LOC 24 N 12^0 00' 12'' E 7^0 55' 13'')

The medium grained Granite petrographically contains quartz, feldspar and mica as major minerals occurring as enhedral and subhedral crystals in a more or less equigranular pattern.

Quartz appears as white to yellowish depending on the orientation of the thin section, its about 40% of the thin section. Plagioclase Feldspar constitute about 35% to 40% of the specimen it appears colourless under plane polarised light and brownish with its characteristic twining when observed under cross polarized light as in Plate 5.

Biotite appears as brown in colour and its about 15% The minor minerals are mostly opaque probably iron oxide occurring in its characteristic cubic shape as in Plate 6.

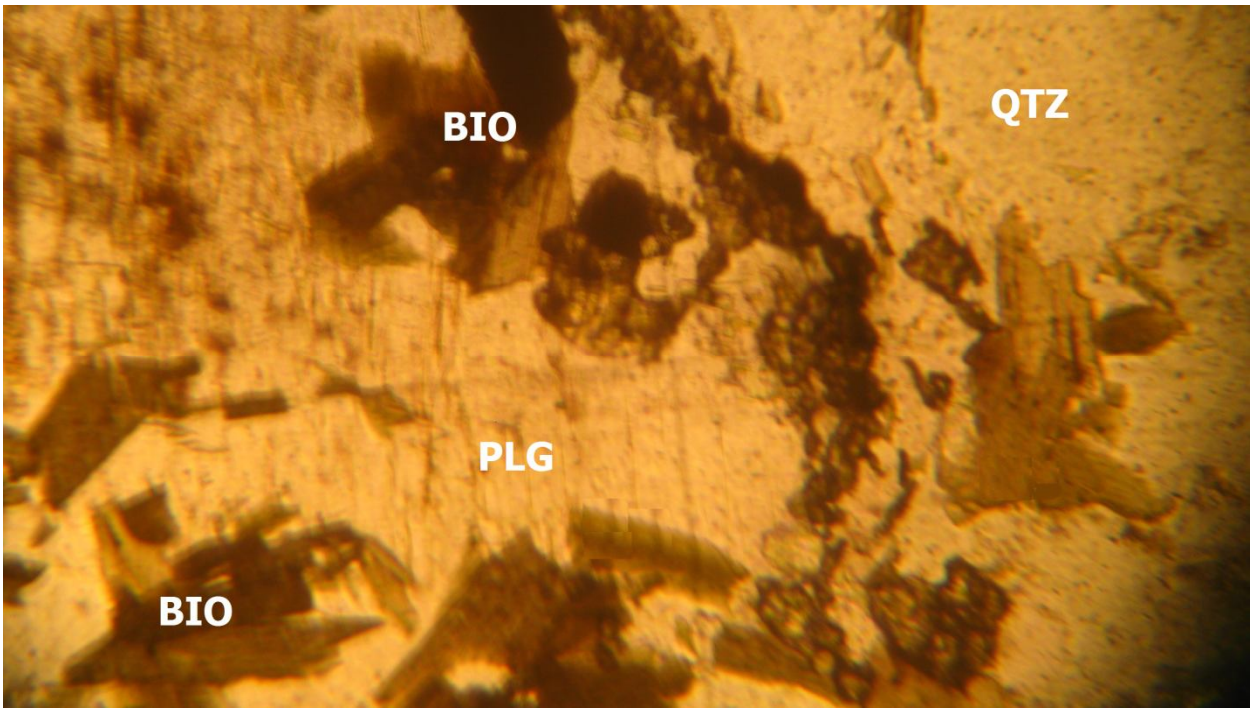


Plate 5 Photomicrograph of granite Sample no. 22. showing subhedral biotite (BIO) and enhedral quartz (QTZ) and Plagioclase feldspar ppl x 25

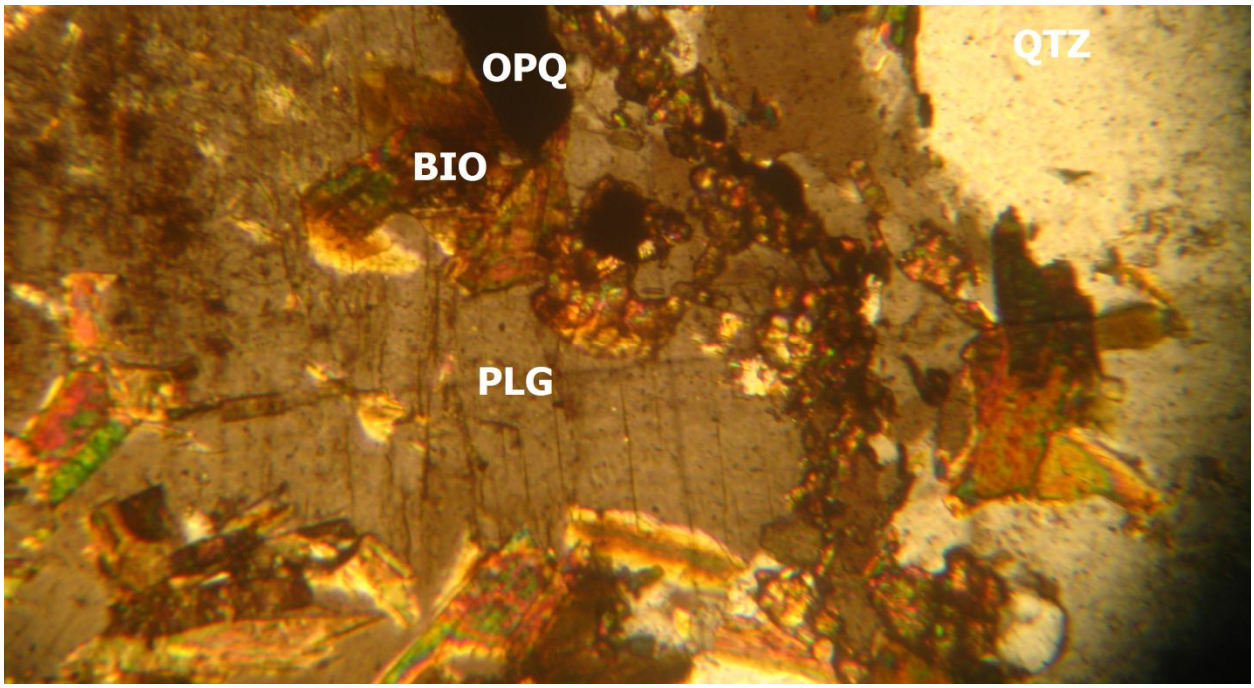


Plate 6. Photomicrograph of granite Sample no. 22 showing subhedral biotite (BIO) and enhedral Quartz (QTZ) Plagioclase feldspar (PLG) and the opaque mineral (OPQ) xpl x 25

3.3 DIORITE (LOC 10 N 12^0 01' 54'' E 7^0 58' 55'')

Diorite occurs as boulders which intrude the fine grained granite. It outcrops as low lying ridges near Shanono along Gwarzo - Shanono road. It account for less than 1% of the rocks in the study area as in Fig 6.



Plate 7 Photograph of Diorite boulders near shanono

In hand spacemen its medium grained. unfoliated rock but when observed under microscope (thin section No JS 3) composed mostly of plagioclase feldspars, hornblenede, epidote, biotite, and quartz.

These minerals occur as idiomorphic and hypidiomorphic grains. Plagioclase feldspar occurs as elongate and prismatic crystals, the characteristic plagioclase twining is evident under cross polarised light (Plate 9), in other places biotite also occur as inclusion within them.

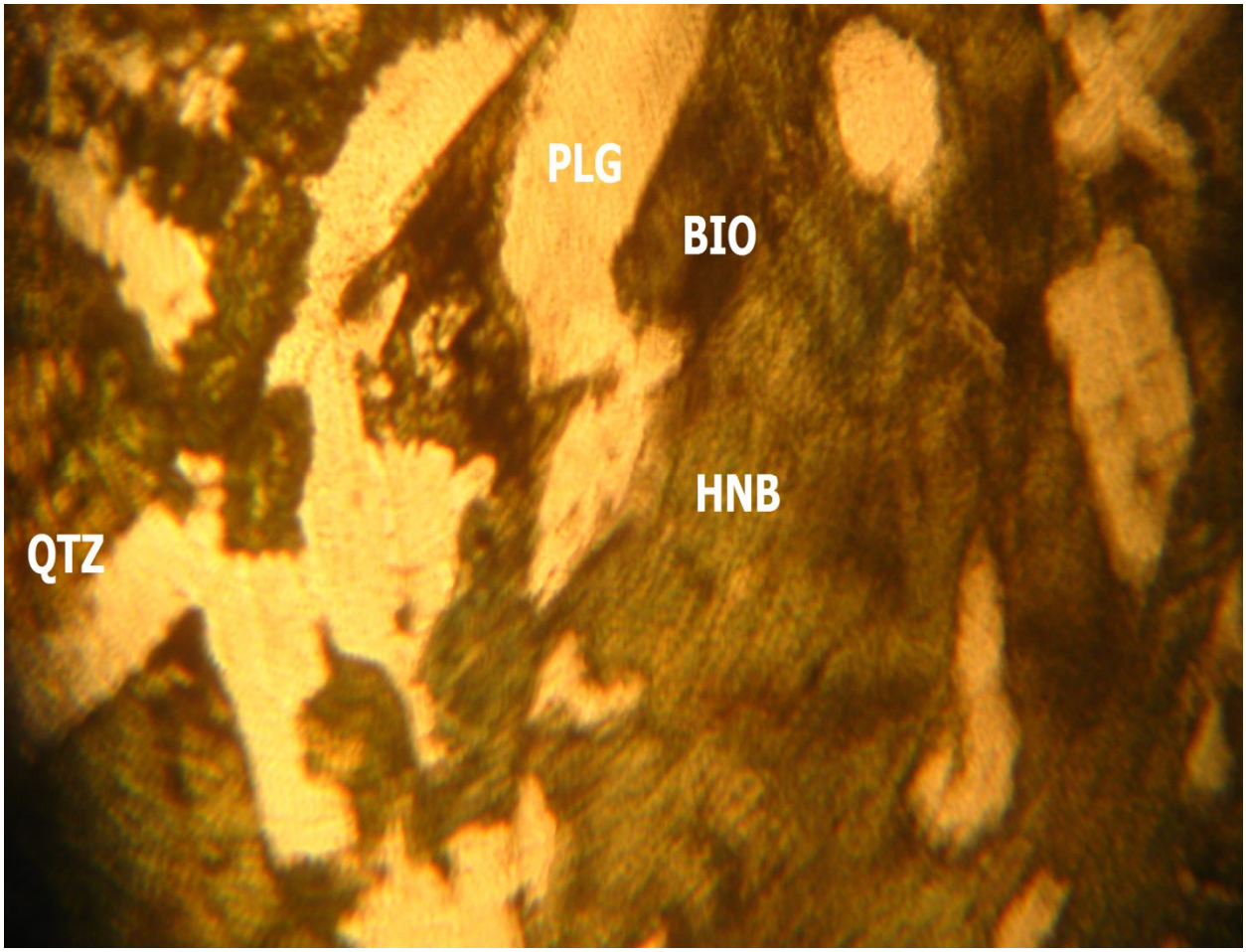


Plate 8 Photomicrograph of diorite Sample no 12 showing idiomorphic and hypidiomorphic minerals arrangement of biotite (BIO) hornblende (HNB) quartz (QTZ) and plagioclase feldspar (PLG) ppl x 10.

Hornblende constitute about 30% of the rock and occurs as pale to dark green mineral in form of heaves with its characteristic parallel cleavage exhibiting high interference colours (Plate 8).

Epidote occurs as light patches lacking cleavage which distinguishes it from hornblende. The crystals are not well formed and occurs as masses between hornblende and plagioclases and constitute about 5% of the sample. Biotite occurs as small brownish patches in various places within the rock and constitute about 7% of the specimen. Other minerals present in minute quantities are quartz and microcline that occurs as accessories within the rock.

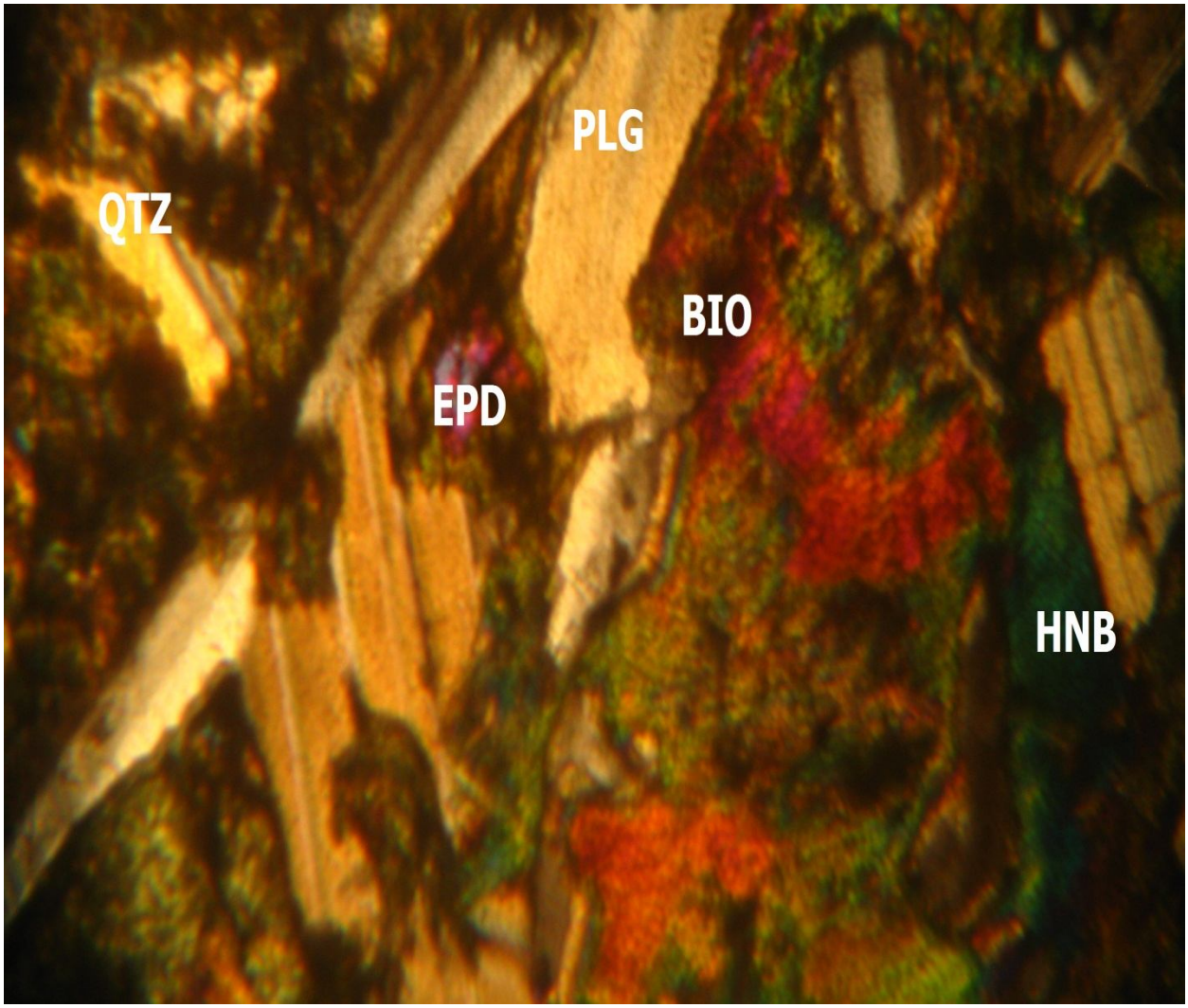


Plate 9 Photomicrograph of diorite Sample no 12 showing subhedral and enhedral minerals of hornblende (HNB) plagioclase feldspar (PLG) quartz (QTZ) biotite (BIO) epidote (EPD) xpl x 20

3.4 QUARTZ-TOURMALINE ROCK (LOC 40: N 12^0 00' 27'' E 7^0 57' 21'')

The Quartz-tourmaline rock occurs throughout the study area as low lying ridges along the shear zone trending in the N-E direction in some places they are about 200 meters long and 2 meters wide and appears as massive bodies which are usually fractured in (Plate 10).

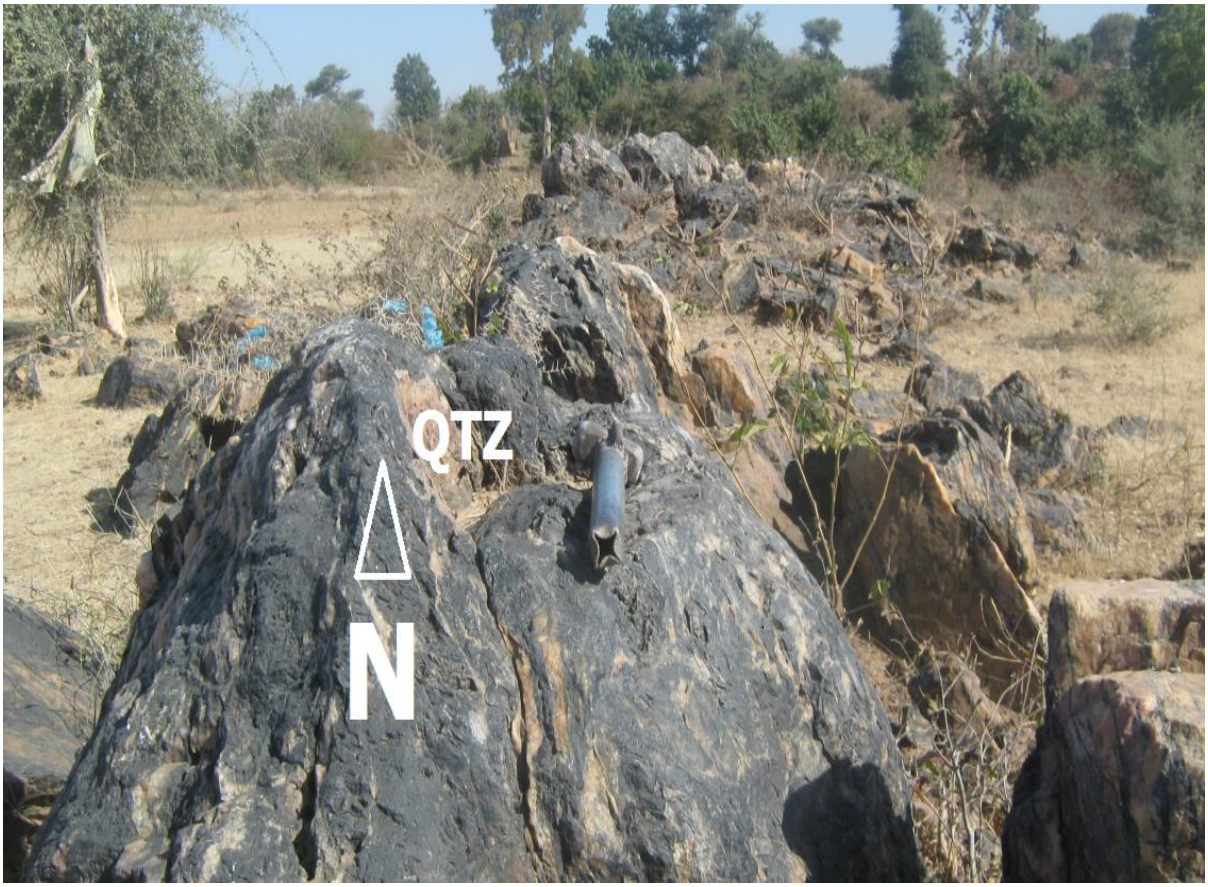


Plate 10 Photograph of quartz-tourmaline rock in massive form and highly fractured

In hand spacemen it appears as massive rock but when observed under microscope (thin section No JS4) is granular (containing small quartz crystals as inclusions) as in Plate 11. Some section of the thin section exhibit clear foliation defined by parallel arrangement of boitite in between tourmaline crystals as Plate 13.

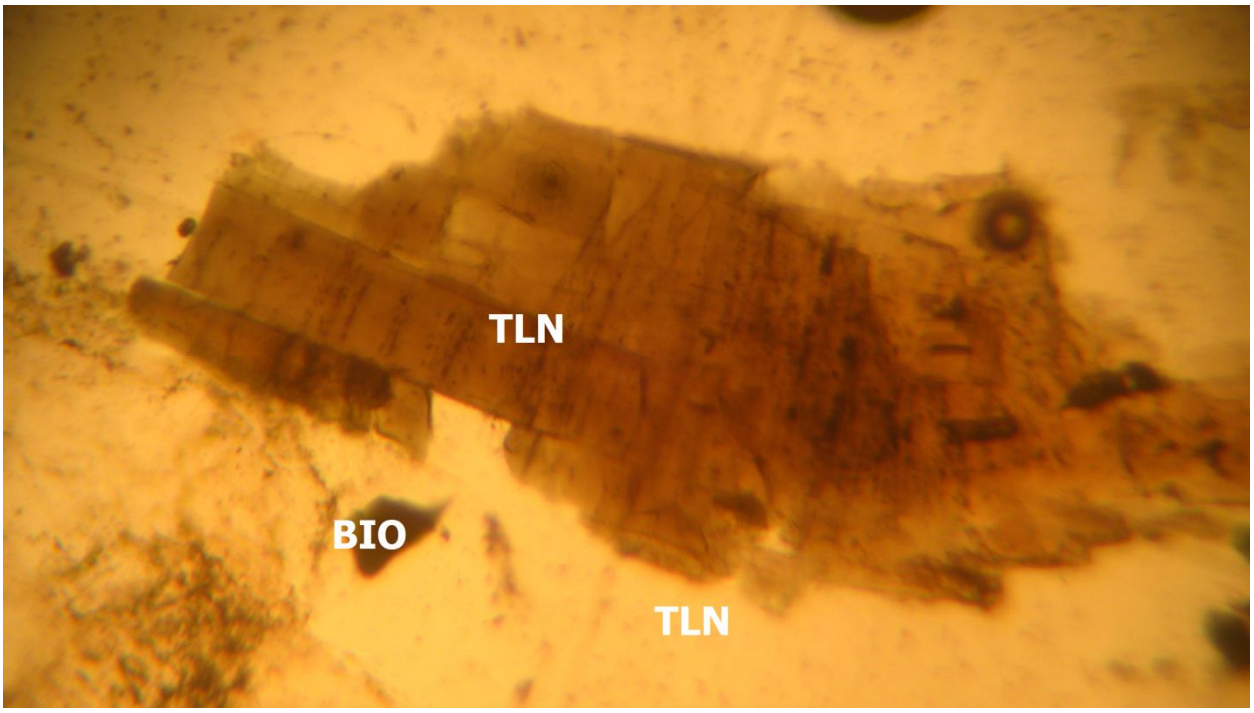


Plate 11 Photomicrograph of quartz-tourmaline sample no 45 showing poikiloblastic textures of biotite (BIO) yellow to brownish tourmaline ppl x 15

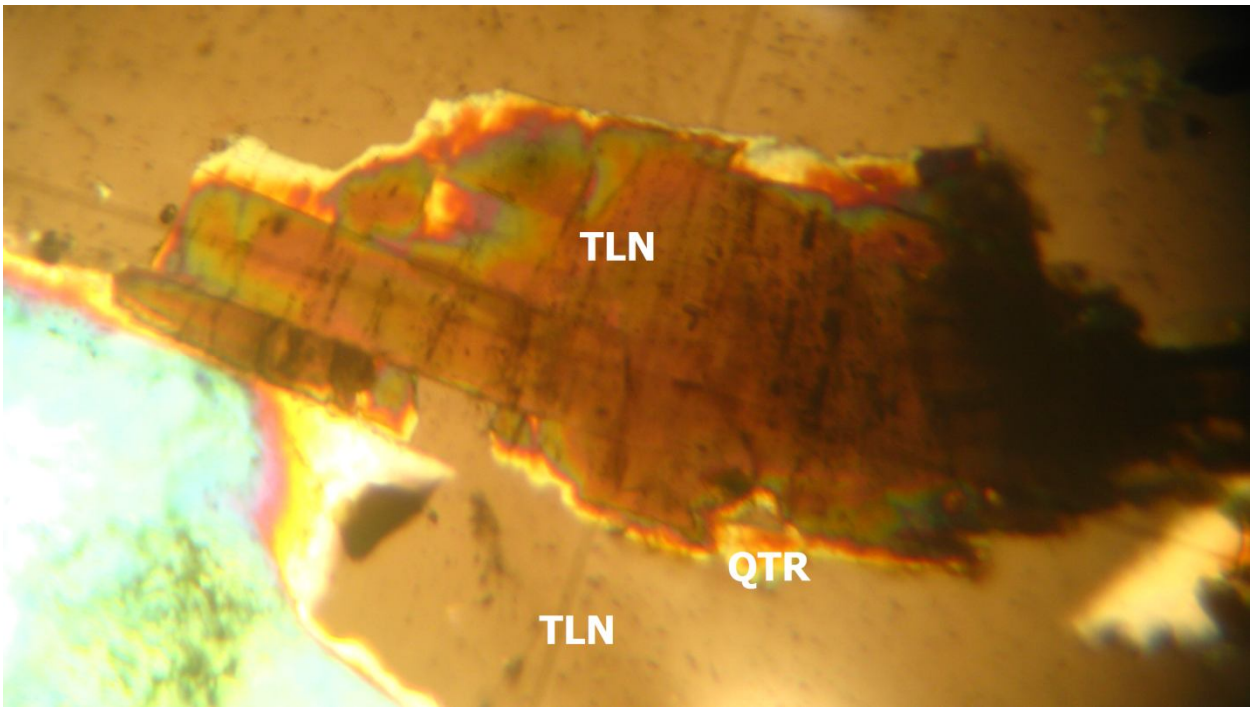


Plate 12 Photomicrograph of quartz-tourmaline sample no 45 showing tourmaline (TLN) and quartz (QTZ) xpl x10

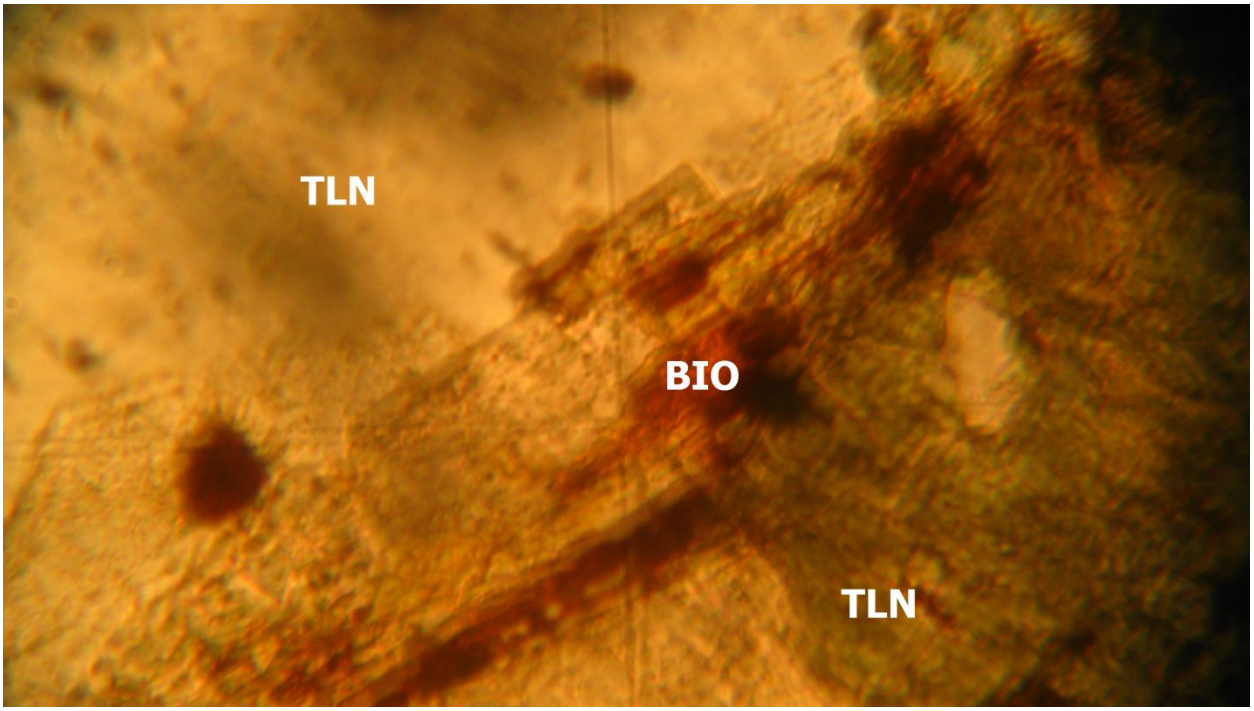


Plate 13 Photomicrograph of quartz-tourmaline sample no 45 showing foliation defined by subparalell alignment of biotite (BIO) within greenish to brownish tourmaline. ppl x 10

Tourmaline under plane polarized light, its bluish to grey when its cut longitudinally with distinctive zoning but when its cut vertically it appears yellowish. The specimen contains 70% of tourmaline defined by biotite inclusion as in Plate 13.

Quartz appears colourless under plane polarized light. It's about 25% of the specimen

Biotite occurs as fine crystals, constituting about 30% of the rock.

Some of the thin sections were examined using transmitted light and under cross polarized light tourmaline is bluish to grey with its distinctive twining as in Plate 17 and quartz appears colourless under plane polarized as Plate 14 and black under cross polarized light with undulose extinction and in some places with vug indicating replacement or formation under low temperature probably epithermal as in Plate 15.

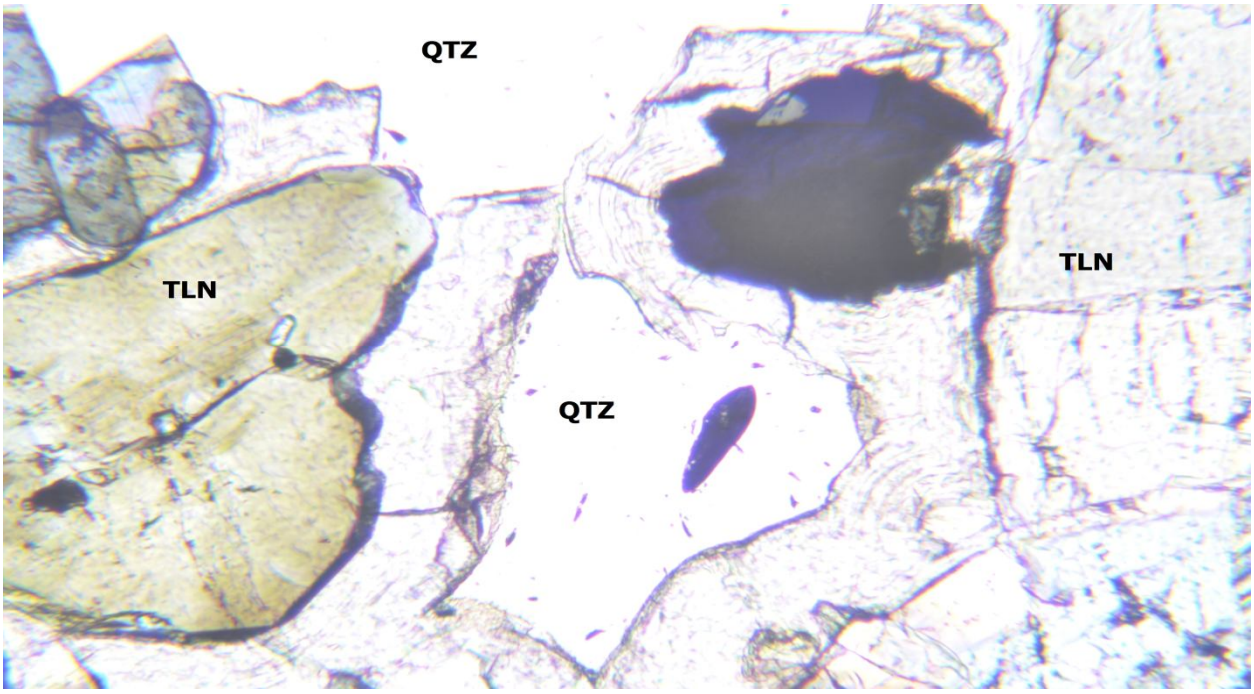


Plate 14 Photomicrograph of quartz-tourmaline sample no 45 showing zoned tourmaline (TLN) and quartz (QTZ) ppl x20

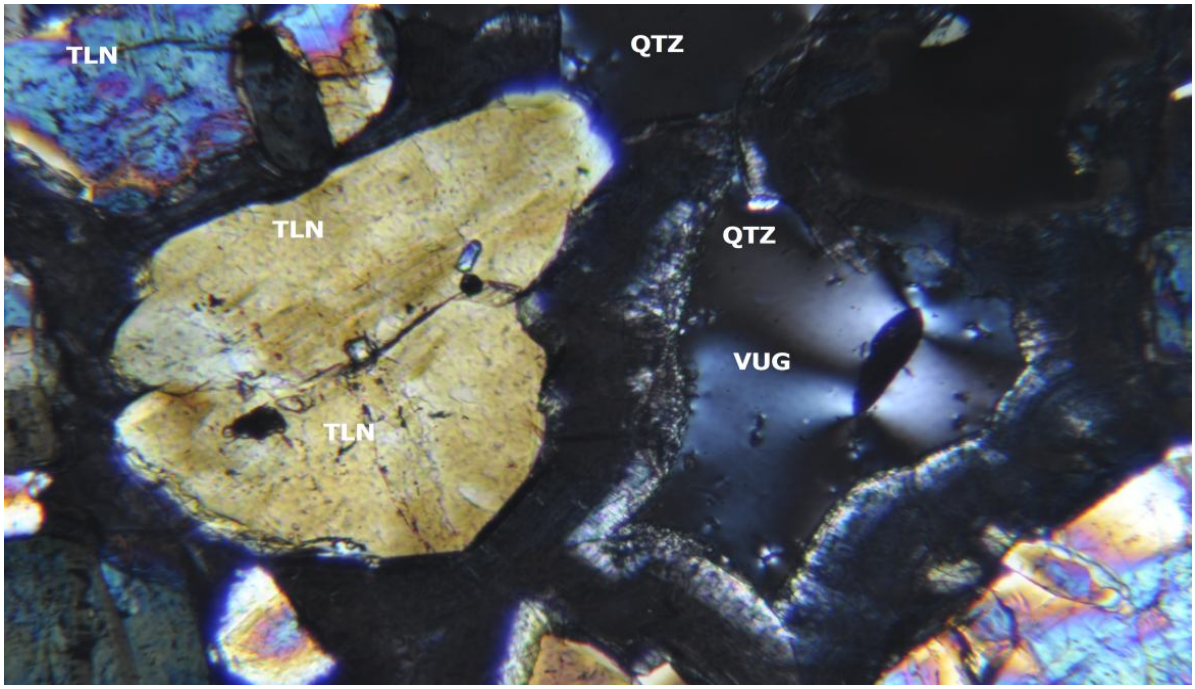


Plate 15 Photomicrograph of quartz-tourmaline sample no 45 showing tourmaline (TLN) quartz (QTZ) and vug (VUG) xpl x20.

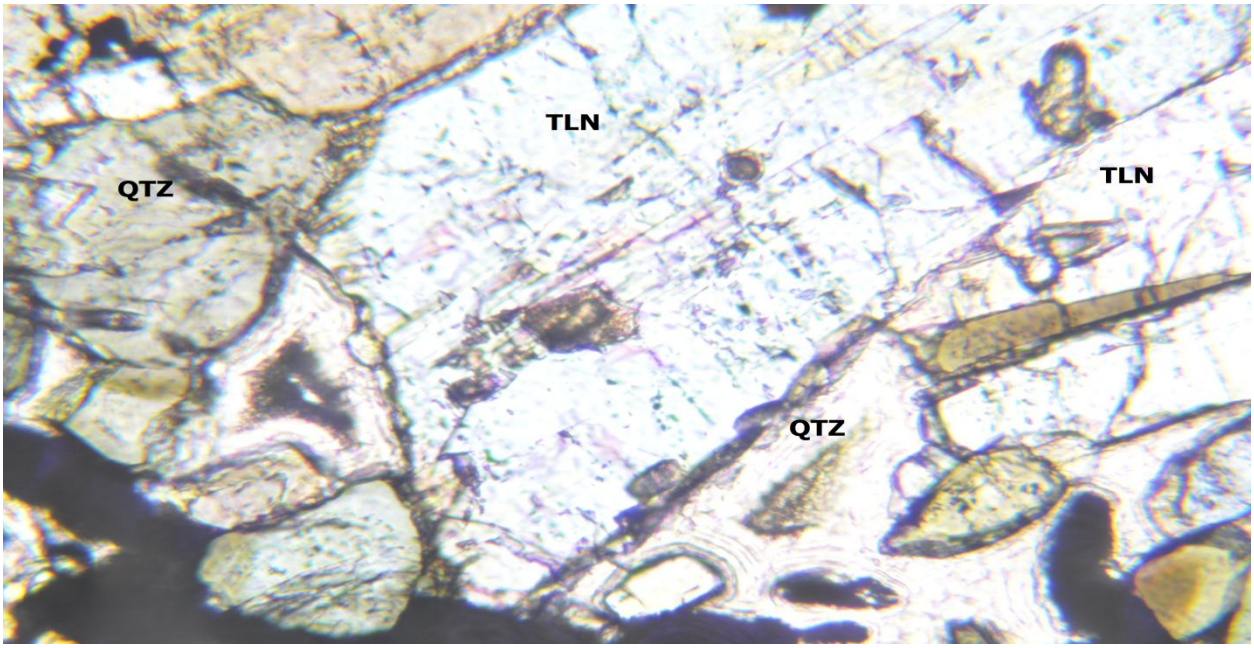


Plate 16 Photomicrograph of quartz-tourmaline sample no 45 showing tourmaline (TLN), quartz (QTZ) and vug (VUG) ppl x15

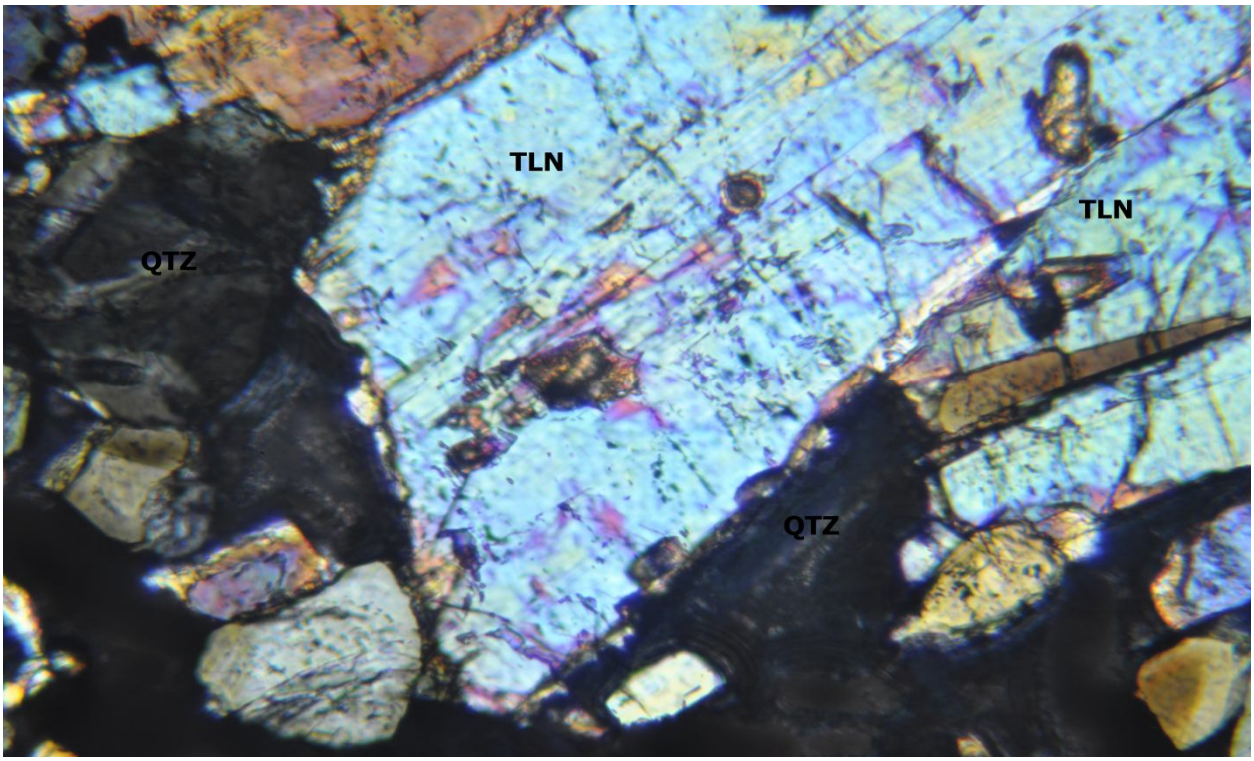


Plate 17 Photomicrograph of quartz-tourmaline Sample no 45 showing tourmaline (TLN) and quartz (QTZ) xpl x15

The thin section samples from Dutsen Danbokoshi were observed under cathodoluminescence have shown tourmaline with its characteristic twining in brown to green and quartz in black colours as in Plate18

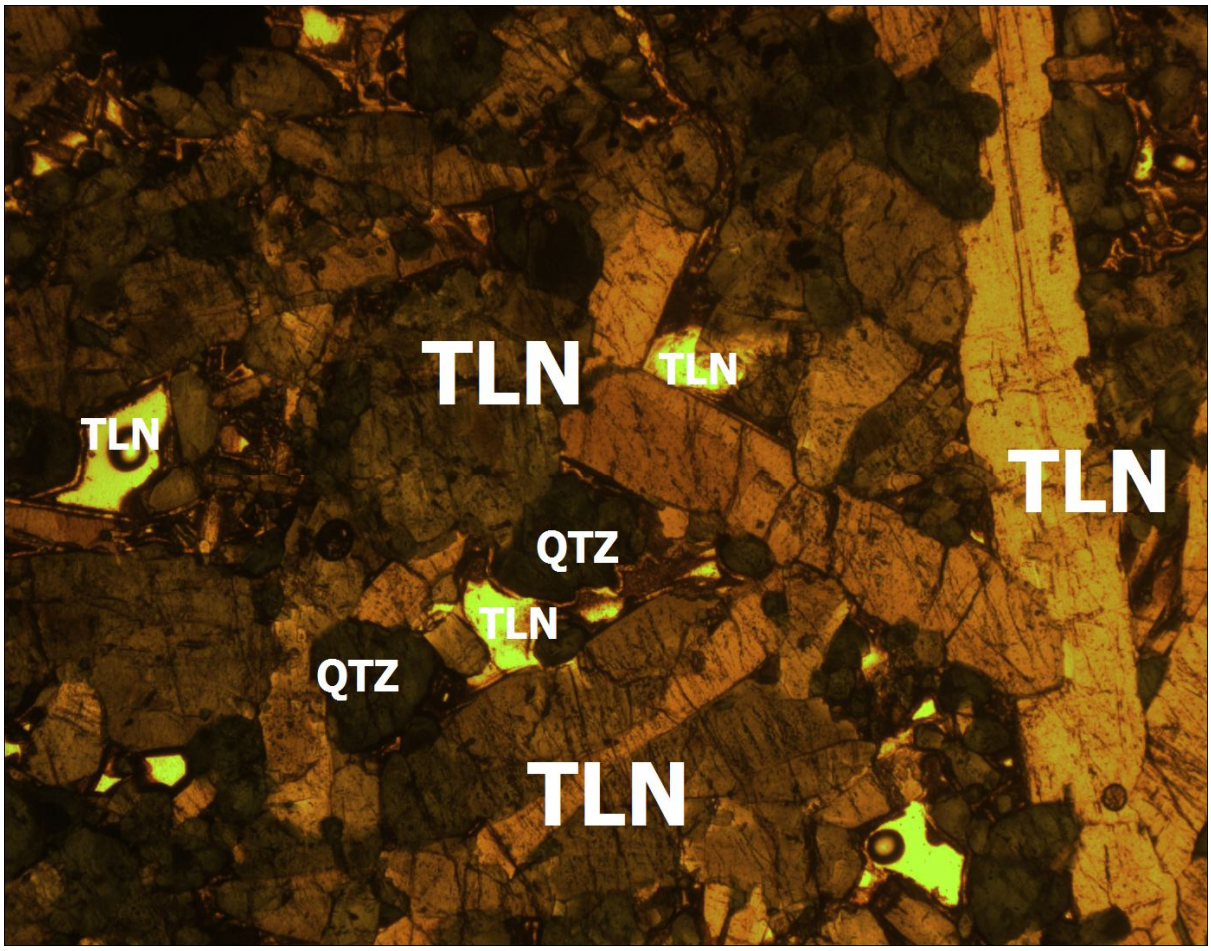


Plate 18 Photomicrograph of quartz-tourmaline sample no 50 showing tourmaline (TLN), Quartz (QTZ).

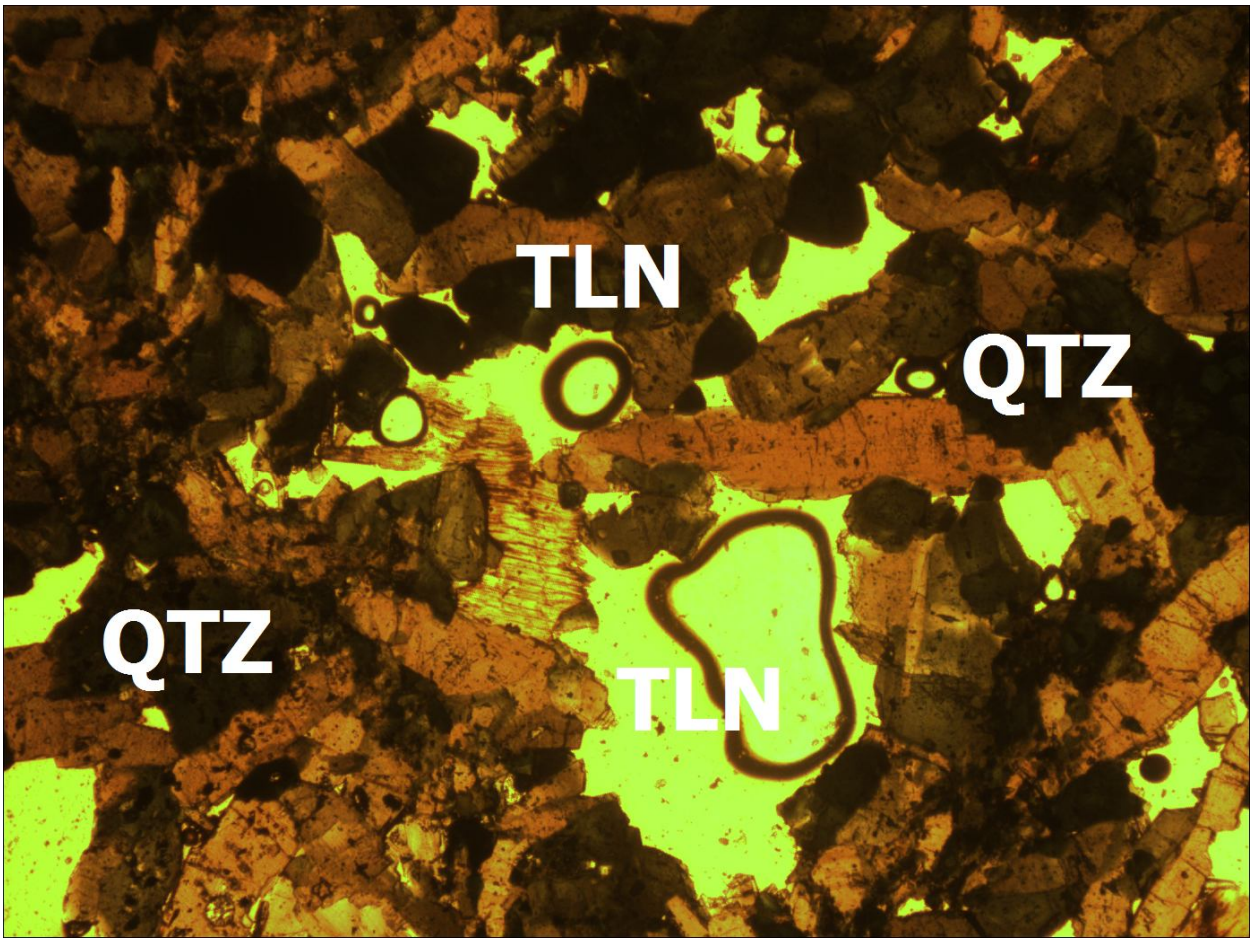


Plate 19 Photomicrograph of quartz-tourmaline sample no 50 showing tourmaline (TLN) and quartz (QTZ)

3.5 QUARTZITE ROCK (LOC 5 N 12^0 00' 24' E 7^0 58' 05'')

Like the quartz-tourmaline quartzite occur throughout the study area as low lying ridges within the sheared zone. In places it appears as massive bodies that are highly fractured as Plate 20



Plate 20 Photograph of quartzite in massive form and highly fractured

In hand specimen the quartzite occurs as massive granular unfoliated rock which when observed under microscope appears as equigranular enhedral quartz crystals with sugary texture (Plate 21).

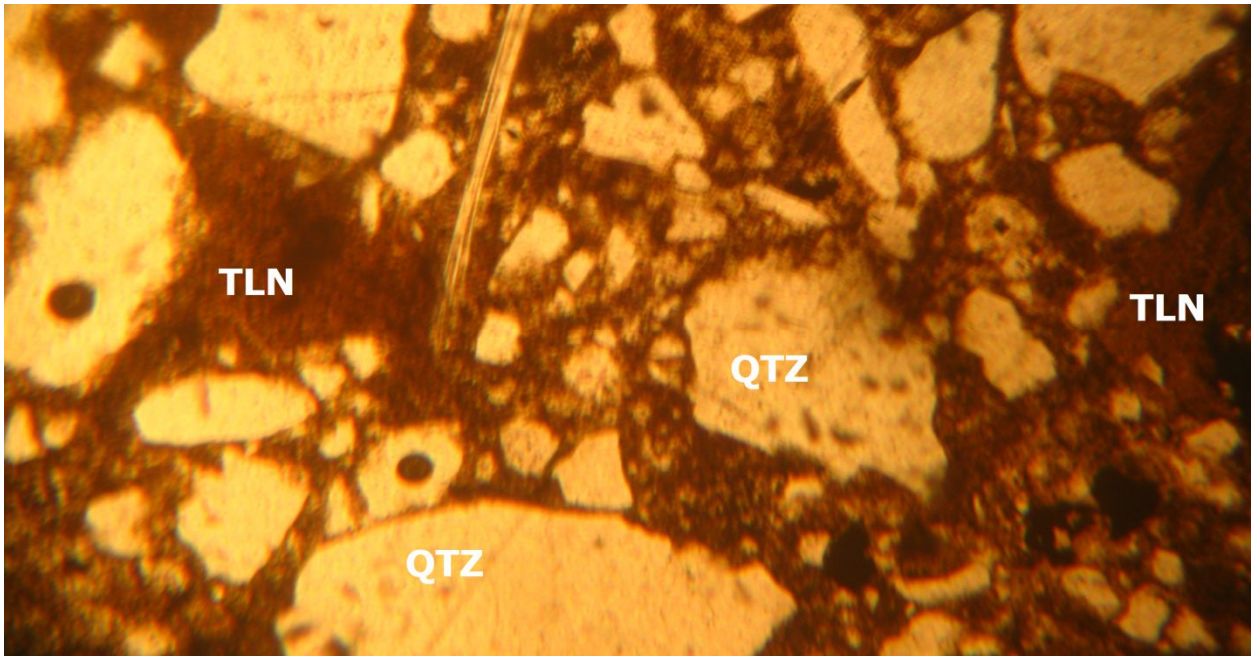


Plate 21 photomicrograph of quartzite sample no. 30 showing quartz (QTZ) inter bedded with tourmaline crystals (TLN) ppl x 15

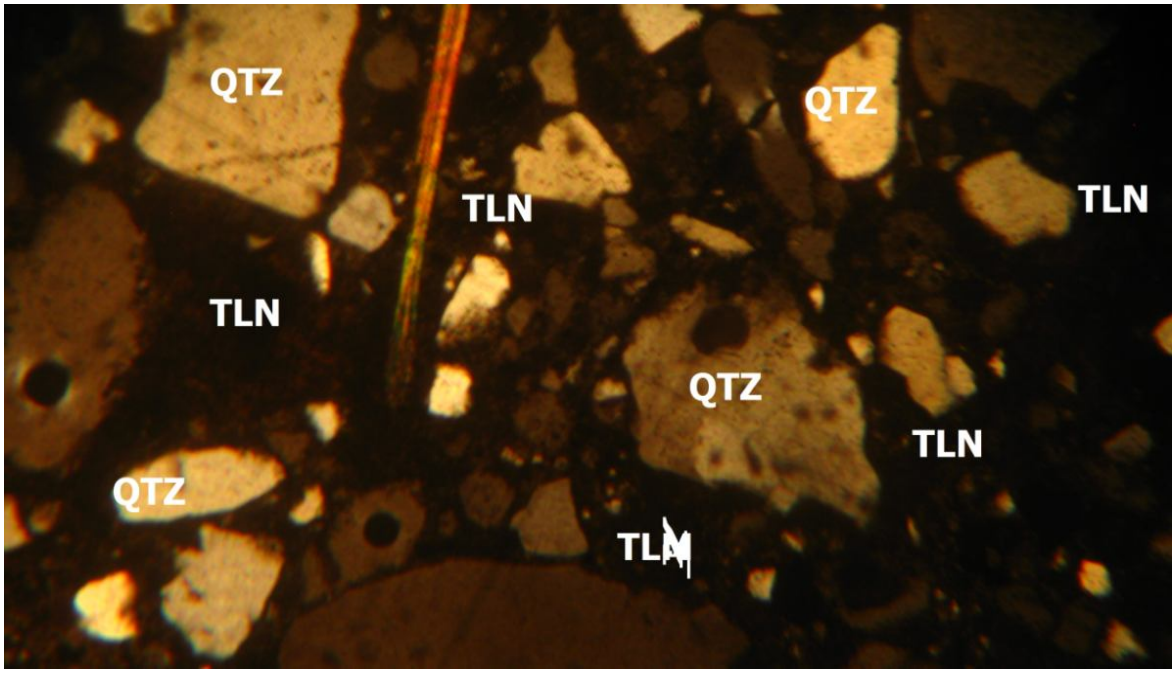


Plate 22 Photomicrograph of quartzite sample no. 30 showing quartz (QTZ) interbedded with tourmaline crystals (TLN) xpl x 20

3.6 METASANDSTONE (LOC 13 N 12^0 01' 19'' E 7^0 56' 10'')

The Metasandstone is found in the western portion of the study area on the Dutsen Danbakoshi Hill, this unit account for about 3% of lithologic unit in the study area and is highly weathered. The insitu sandstone occurs in bedded unit ranging from 5 to 8cm thick as in fig 6.



Plate 23 Photograph of Metasandstone showing the effect of weathering

In hand specimen its medium grained rock and appears pinkish to dark grey in colouration, but when observed under microscope (thin section JS 7) composed mostly of quartz grains of various sizes cemented by a feldspartic cementing medium that is very fine grain as in plate 25, Some of the layer of quartz grain exhibit fractures indicting deformation.

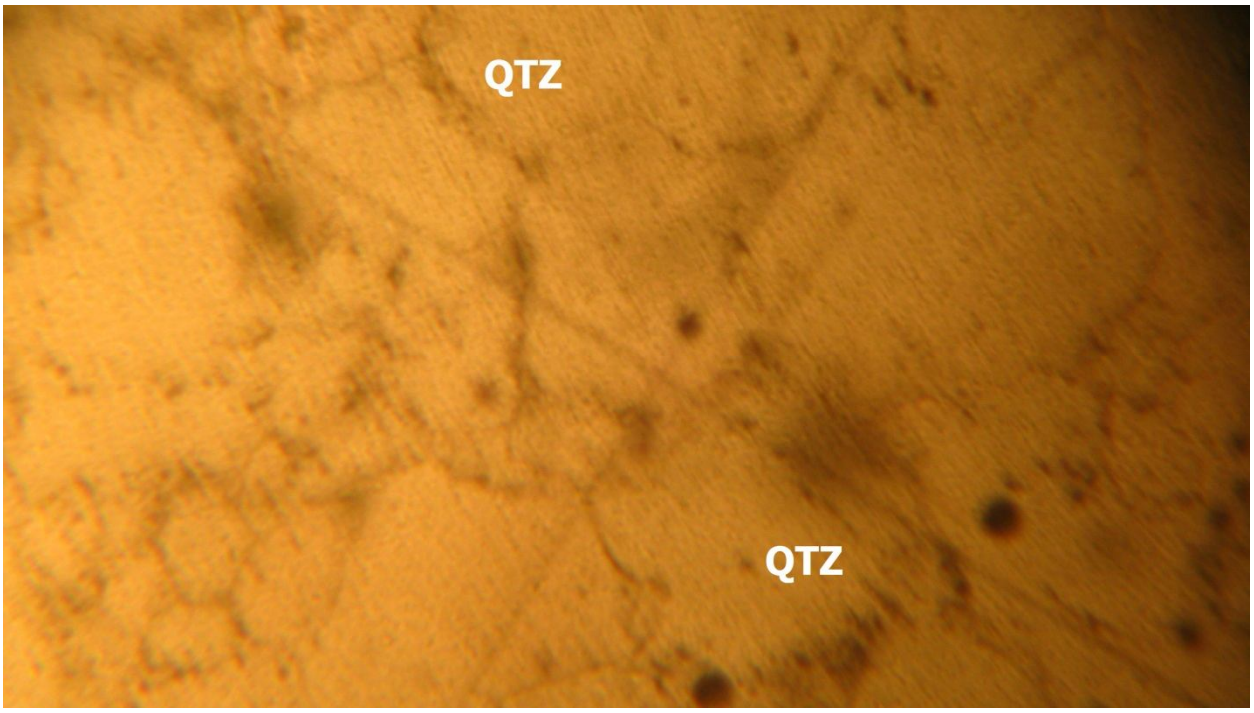


Plate 24 Photomicrograph of Metasandstone sample no. 25 showing quartz crystals In yellowish colour ppl x 10

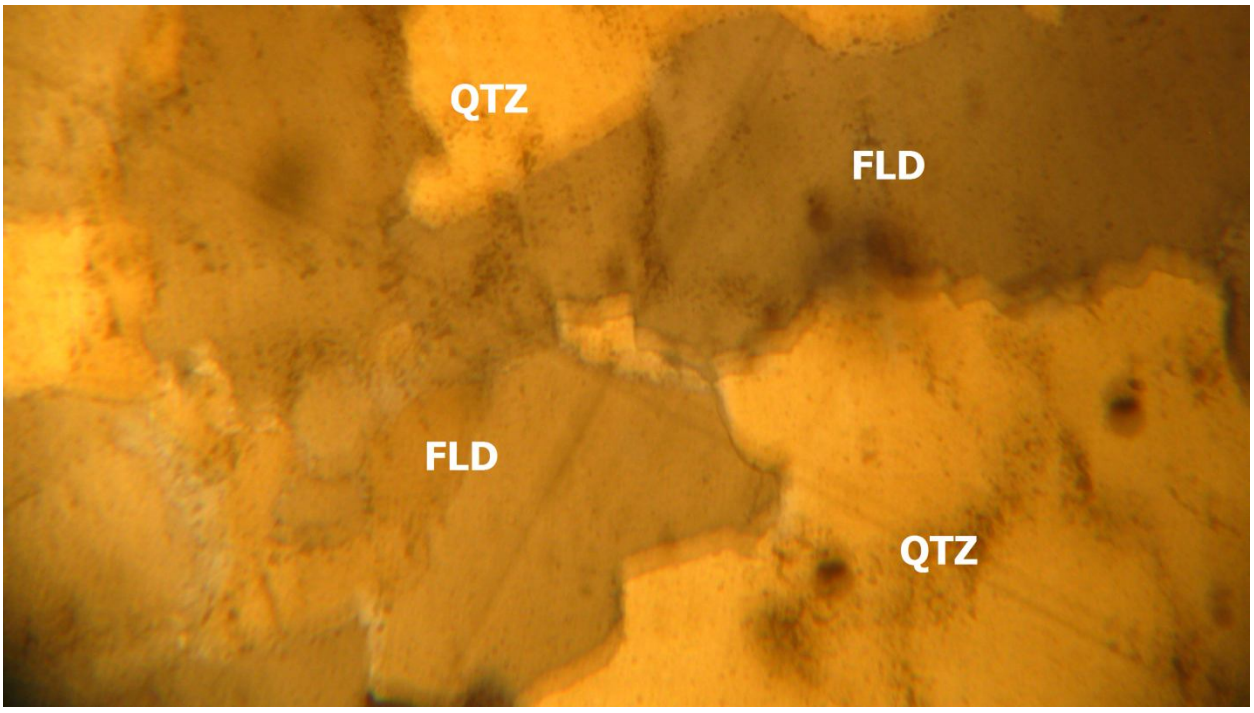


Plate 25 Photomicrograph of Metasandstone sample no. 25 showing quartz crystals (QTZ) and feldspar (FLD) Xpl x 10

CHAPTER 4

STRUCTURAL GEOLOGY

4.1 Preamble

The Dutsen Danbakoshi area is located in the North-eastern part of Malumfashi schist belt in sheet 56 Musawa S.E. Two structural trend can be inferred in the study area, the younger joints trending NNW-SSE cross cutting the older joints which trend NNE-SSW directions this coincided with early structural trend found in the basement adjacent to Birnin Gwari belt where the original granodiorites were sheared to form the Zungeru Mylonites in two belts on either side of parallel to the schist belt Fitches et. al., (1985).

The geological structures such as joints and shears found in the study area serve as conduit for the fluid to come to the surface in the shear zone were the tourmalinization takes place.

4.2 Shears

Shears are conspicuous along Quartz-tourmaline ridges an example is in the shear zone which contain the Quartz-tourmaline as in Plate 26 outcrop at location 20 latitude 12^0 02'06'' N, 07^0 56' 32'' E. It has a general north-south trend and might result from a stress acting in a general direction north east-south west.



Plate 26 Photograph Showing the Fractured nature of Quartz-tourmaline ridge at loc. 20 N 12^0 02' 06'' E 07^0 56' 32''.

4.3 Joints

Joints are the most abundant structural features observed and are present in most of the rock exposures. However the granitic rocks displayed a jointing pattern with a dominant NNE – SSW following the general North – South trend. In several places the younger joints trending NNW-SSE were found cross cutting the older ones trending NNE-SSW.

.

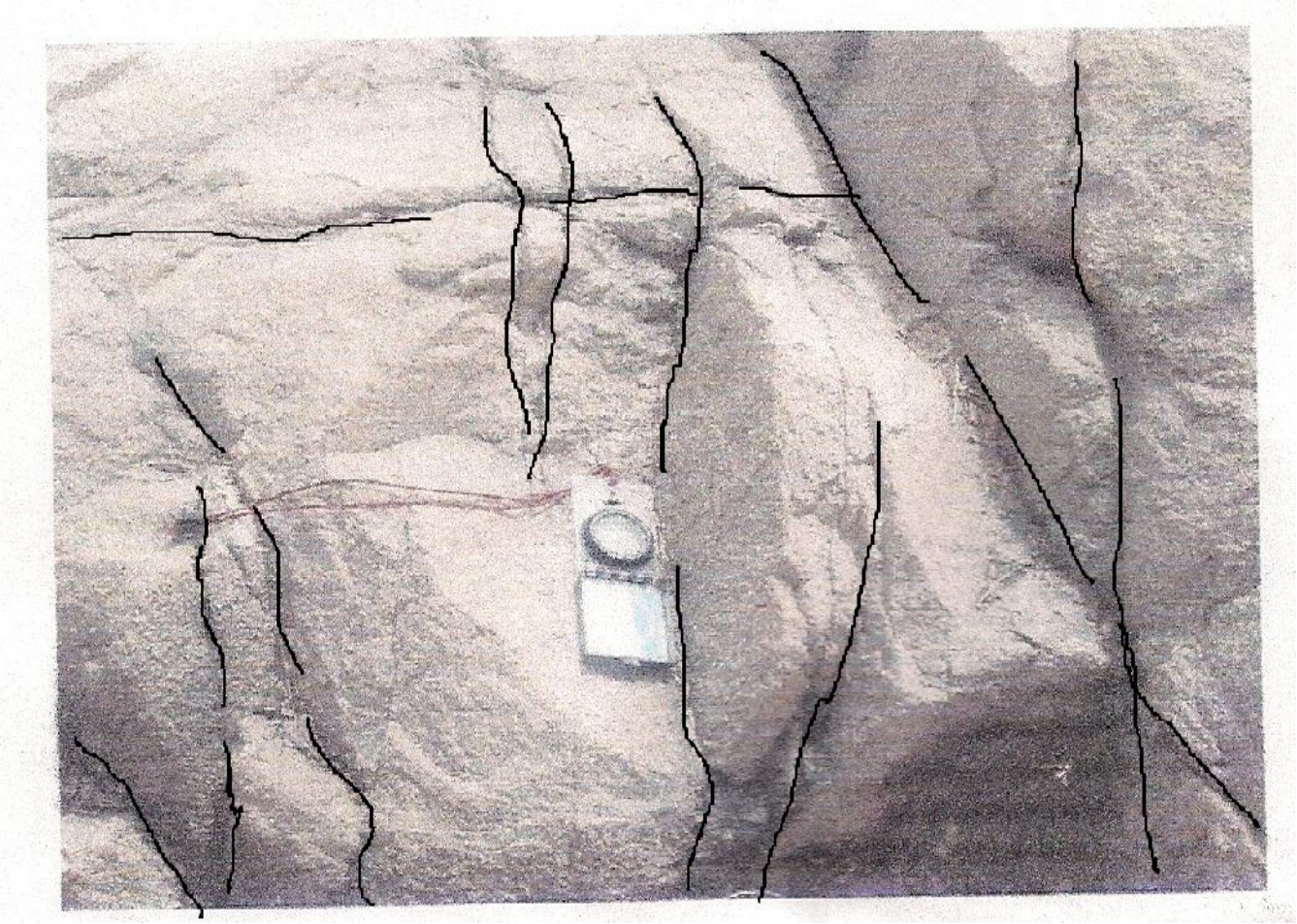


Plate 27 Photograph of joints geometry as observed in medium grained granite at loc. 21 N 12^0 00’ 79’’ E 07^0 59’ 39’’ of the study area.

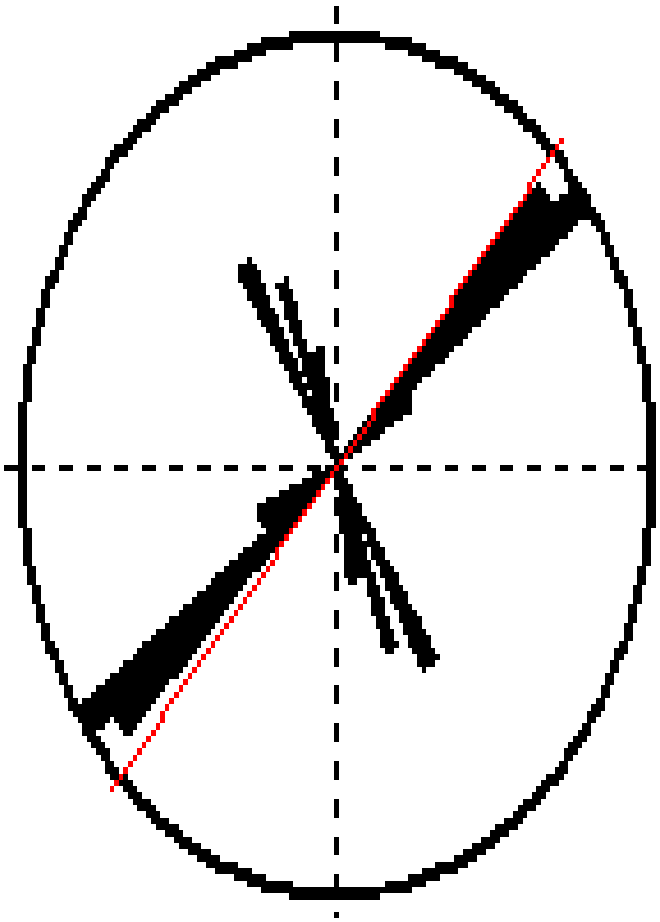


Fig. 4.0 Rose diagram of joint trends in the medium grained granite

The rose diagram of joints in the medium grained granite indicating the presence of two major stresses is in NNE-SSW direction while minimum stress is in the NNW-SSE direction (Fig 4)



Plate 28 Photograph of joints geometry as observed in the medium grained Granite at loc. 30 N 12^0 01’ 34’’ E 07^0 56’ 11’’

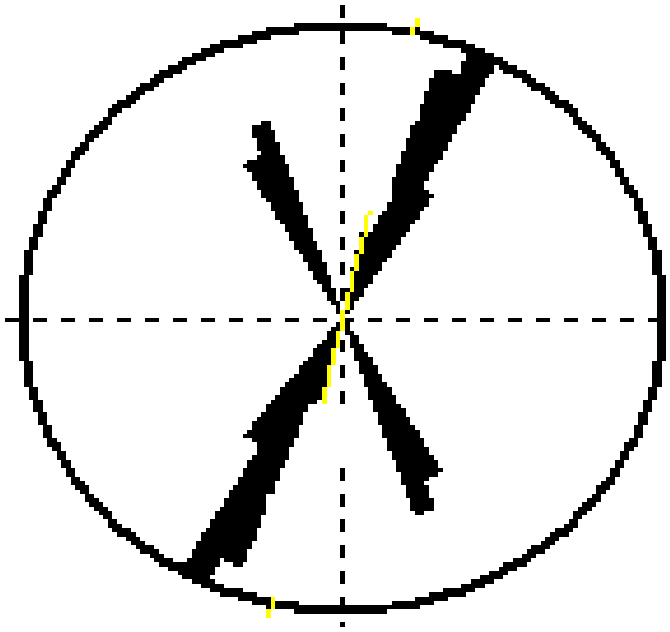


Fig. 4.1 Fig. 4.0 Rose diagram of joint trends in the medium grained granite

The rose diagram of joints in the medium grained granite indicating the presence of two major stresses is in NNE-SSW direction while minimum stress is in the NNW-SSE direction (Fig 4.1)

Chapter 5

GEOCHEMISTRY

5.1 Sample Collection and Analytical Techniques.

Twenty one representative rock samples collected from Dutsen Danbakoshi were used in this study. Seventeen samples were sent for whole rock geochemical analysis, while four samples were sent for boron isotope ($\sigma\ ^{11}B$) analysis. Sample of basement complex rock (eight Granitic rocks MK01, MK02, MK03, MK04, MK05, MK06 MK07, MK08 and four Diorite MK09, MK10, MK11 MK12) and five Quartz-tourmaline (MK013, MK14, MK15, MK16, MK17) were subjected to whole rock analysis and four Quartz-tourmaline (MK18, MK19, MK20, MK21) were analyzed for boron isotope $\sigma\ ^{11}B$.

The rock samples were crushed and pulverized into fine powder, packed into polythene bags at the sample preparation laboratory of the Department of Geology, Ahmadu Bello University, Zaria, The chemical analysis was done at Activation laboratories (Actlabs), Ancaster, Ontario, Canada, Nigerian Geological Survey Agency Kaduna for major, trace elements concentrations, and ALS Scandinavia Lulea Sweden for boron isotope determination

The analytical methods used in this study by the Activation laboratories (Actlabs), Nigerian Geological Survey Agency Kaduna and ASL Scandinavia are inductively coupled plasma mass spectrometry (ICP-MS), X-Ray Fluorescence for major, trace, and rare earth elements analysis and inductively coupled plasma sector field mass spectrometry (ICP-SFMS) for boron isotope analysis. Major elements are reported in weight percent (wt ‰) and trace elements were reported in parts per million (ppm)

An X-Ray Florescence (XRF) spectrometer is an X-ray Instrument used for routine relatively non-destructive chemical analysis of rocks, minerals, sediments and fluids. It works on wavelength-dispersive spectrospic principal that are similar to an Electron Probe micro Analyser (EPMA). It is typically used for bulk analyses of large fractions of geological materials. The relative ease and low cost of sample preparation, and the stability and ease of use of X-ray spectrometers make this one of the most widely used methods for analysis of major and trace elements in rocks, minerals, sediment

The analysis of major and trace elements in geological materials by XRF is made possible by the behavior of atoms when they interact with X-radiations. An XRF spectrometer works because if a sample is illuminated by an intense X-ray beam, known as the incident beam, some of the energy is scattered, but some is also absorbed within the sample in manner that depends on its chemistry. The incident X-ray beam is typically produced from a Rh target, although W, MO, Cr and other can also be used depending on the application.

When this primary X-ray beam illuminates the sample it is said to be excited. The excited sample in turn emits X-ray along a spectrum of wavelengths characteristics of the types of atoms present in the sample.

X-ray fluorescence is particularly well suited for investigations that involves

Bulk chemical analysis of major elements (Si, Ti, Al, Fe, Mn, Mg, Ca, Na, K, P) in rock and sediment.

bulk chemical analysis of trace elements (>1 ppm, Ba, Ce, Co, Cr, Cu, Ga, La, Nb, Ni, Rb, Sc, Sr, Rh, U, V, Zr, Zn) in rock and sediment.

In theory the XRF has the ability to detect X-ray emission from virtually all elements depending on the wavelength and intensity of incident X-rays. However in practice, most commercially available instruments are very limited in their ability to precisely and accurately measure the abundances of elements with $Z < 11$ in most natural earth materials. XRF analyses cannot distinguish variation among isotopes of an element, so these analyses are routinely done with other instruments such as SIMS and TIMS. XRF analyses cannot distinguish ions of the same element in different valence states, so these analyses of rocks and minerals are done with techniques such as wet chemical analysis on Mass Bauer spectroscopy.

The ICP-MS instrument measures most elements in the periodic table with detection limits at or below ppt range with exception of these element H, He, C, N, O, F, S, Ne, Ar, Kr, Xe, Rn.

Most analyses performed on ICP-MS instrumentation are quantitative; however it also can serve as an excellent semi-quantitative instrument. By using a semi- quantitative software package, an unknown sample can be analyzed for 80 elements in three minutes, provided semi-quantitative data that is typically within $\pm$ 30% of the quantitative values.

The primary reason for the growing popularity of ICP-MS can be summarized in these points.

Instrument detection limits are at or below the single part per trillion (ppt) levels for much of the periodic table.

Productivity is unsurpassed by any other technique

Isotopic analysis can be achieve red readily

Analytical working range is nine orders of magnitude

An ICP-MS consists of the following components

Sample introduction system- composed of nebulizer and spray chamber and provides the means of getting samples into the instrument.

ICP-torch and RF coil - generates the argon plasma, which serves as the ion source of the ICP-MS

Interface - links the atmospheric pressure ICP ion source to the high vacuum mass spectrometer.

Collision/reaction cell - precedes the mass spectrometer and is used to remove interferences that can degrade the detection limits achieved. It is possible to have a cell that can be used both in the collision cell and reaction cell modes, which is referred to as a universal cell

Ion optics – guides the desired ions into the quadruple while assuring that neutral species and photons are discarded from the ion beam

Mass spectrometer- act as a mass filter to sort ions by their mass-to –change ratio (m/z)

Date handing and system controller – controls all aspects of instrument control and data handling to obtain final concentration results.

Detector- counts individual ions exiting the quadruple

The ICP-MS works when samples are introduced into argon plasmas as aerosol droplets. The plasma dries the aerosol, dissociates the molecules, and then removes an electron from the

components, thereby forming singly-change ions, which are directed into a mass filtering device known as mass spectrometer.

Upon exciting the mass spectrometer ions strike the first dynode of an electron multiplier, which serves as a detector. The impact of the ions releases a cascade of electrons, which are amplified until they become a measureable pulse. The software compares the intensities of the measured pulses to those from standards, which make up the calibration curve, to determine the concentration of the element.

For each element measured, it is typically necessary any to measure just one isotope, since the ratio of isotopes, or natural abundance, is fixed in nature.

ICP-MS can be used to measure the individual isotopes of each element; this capability brings value to laboratories interested in one specific isotope of an element or in the ratio between two isotopes of an element.

5.2 Geochemical Analysis Result

Below are the results of geochemical analysis which include major, trace, rare earth element and boron isotope values of the representative samples as presented in Table 1-4

5.3 GEOCHEMISTRY OF GRANITE

5.3.1 Major elements distribution

The major elements data of granite from the study area are presented in Table1. The SiO_2 content of granite varies from (67.30 – 72.71wt %) with average (70.0171wt %) high alkali – oxide average with Na_2O (2.5916wt %) and K_2O (5.2875wt %) and low average content of CaO (1.9725wt %) and MgO (0.78wt %) while average content of Fe_2O_3 (total) (2.1288wt %)

5.3.2 Trace elements distribution

The geochemical data of the granite shows variation of trace elements table 2.The result shows depletion in average Zirconium (Zr) content of 182 ppm for granitic samples when compared with average crustal composition of 132 ppm Rudnick and Gao (2003). Niobium (Nb) values range from (13 – 34 ppm) enriched when compares to average crustal composition of 8 Rudnick and Gao (2003).

Lithophile elements (K, Ba, Rb, Sr) concentrations can also be used to show the fractionation pattern of these elements in both the host rocks and Quartz-tourmaline rocks. There is enrichment of Ba in granites (0.45 – 1000 ppm) when compared to the average crustal composition of 456 ppm Rudnick and Gao (2003). Rb is markedly enriched (0.38 – 319 ppm) with average 121.655 when compared to crustal average of 49 ppm Rudnick and Gao (2003). There is also depletion of Sr which range from (0.32 – 232) with average of 198 when compared with average crustal composition of 320 Rudnick and Gao (2003).

Yttrium values in the granite are higher (45 ppm) when compared with an average of 40 ppm Y for granite Taylor (1965).

All the REE abundances for granites were normalized after Boynton (1984) and then plotted in Fig. 5.0. The REE fractionation pattern of the granite is characterized by distinct enrichment of light rare earth elements (LREE) and depletion of heavy rare earth elements (HREE). There is a noticeable negative Eu anamoly for all the granitic samples.

Table 5 Chondrite-normalized REE values of granite

Sample No	TmN	YbN	LuN	Eu/Eu*	LaN/ YbN	LaN/ SmN	CeN/ YbN	CeN/ SmN	EuN/ YbN	Sum REE
MK01	4.67	4.55	3.82	0.77	12.33	4.21	8.85	3.02	1.74	81.18
MK02	4	3.64	3.24	0.85	6.83	2.02	12.68	3.75	2.12	69.11
MK03	14.67	13.18	12.35	0.59	9.43	4.35	7.8	3.6	0.97	191.65
MK04	23.67	20.45	20.45	0.5	13.02	4.74	9.12	3.36	1.05	376.9

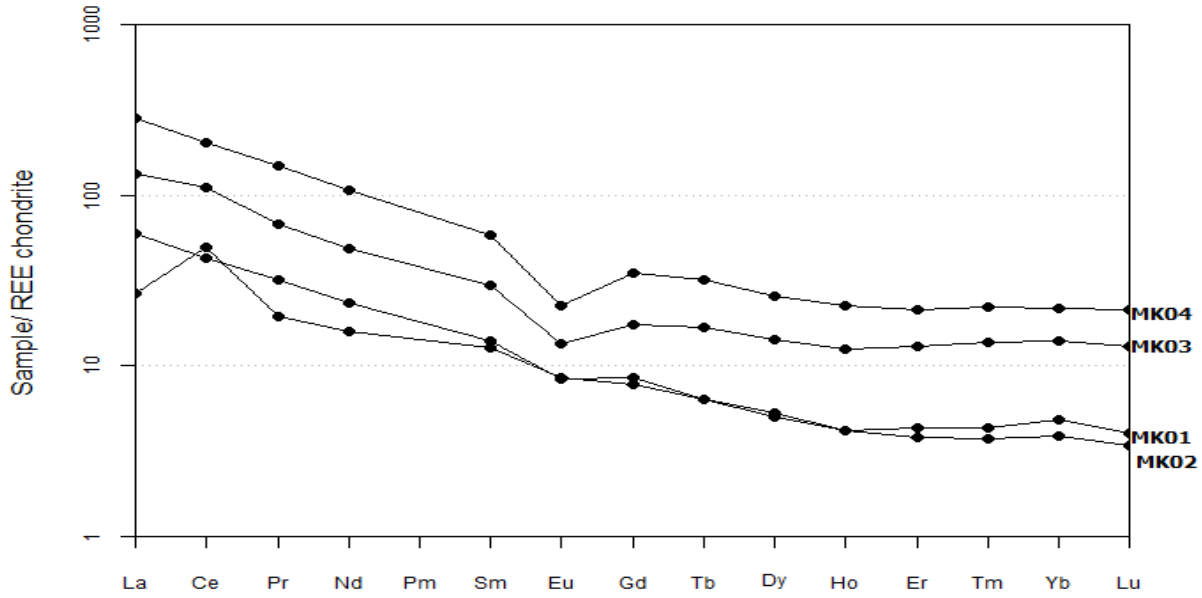


Fig. 5.0 Chondrite-normalized REE patterns for granitic rocks of Dutsen Danbakoshi after Boynton (1984)

5.4 GEOCHEMISTRY OF DIORITE

5.4.1 Major element distribution

The geochemical data obtained on the major elements of Diorite is presented in Table 1. diorite is depleted in SiO_2 content (41.38wt %), but is enriched in CaO (17.1725wt %). There is also significant enrichment of Al_2O_3 (13.823wt %), and Fe_2O_3 (T) (17.475wt %) in the diorite sample.

5.4.2 Trace element distribution

The trace element data of diorite is presented in Table 2, Lithophile elements (K, Ba, Rb, Sr) fractionation pattern in the rock can therefore be determined, thus there is depletion of Ba in diorite (83 ppm) when compared to the average crustal composition of 465 ppm Rudnick and

Gao (2003). There is also depletion of Rb (8.5 ppm) when compared to the mean crustal average of 49 ppm for Rb Rudnick and Gao (2003).

All the REE abundances are normalized after Boynton (1984) and then plotted in Fig. 5.1. The REE fractionation pattern of the diorite is characterized by an enrichment of the (LREE) and depletion (HREE).and weak negative Eu anomaly.

Table 6 Chondrite-normalized REE values of diorite

Sample No	TmN	YbN	LuN	Eu/Eu*	LaN/ YbN	LaN/ SmN	CeN/ YbN	CeN/ SmN	EuN/ YbN	Sum REE
MK05	17.67	15	14.12	0.92	3.41	2.21	2.78	1.8	1.24	102.99

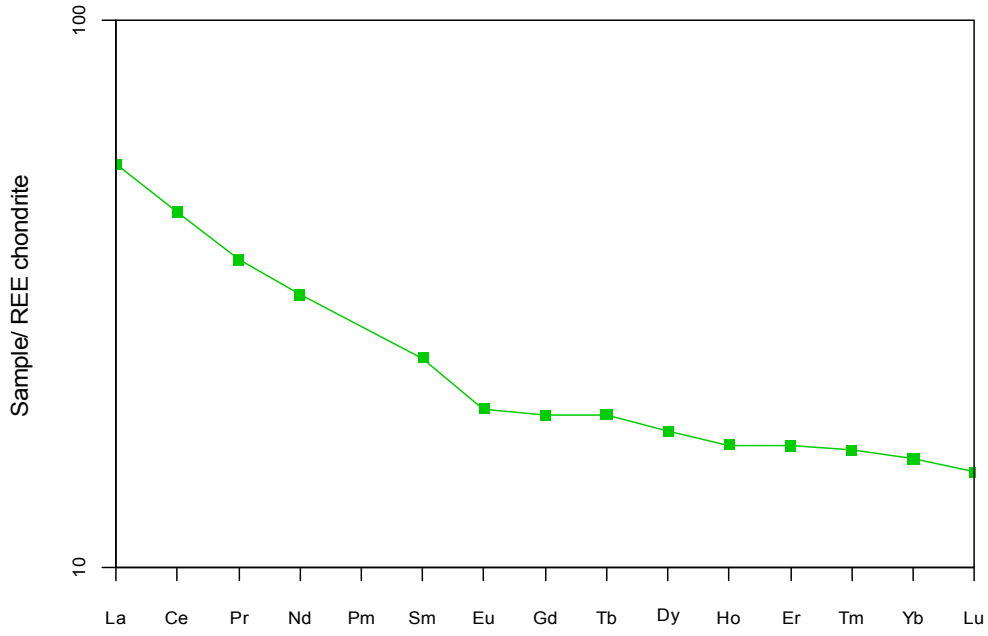


Fig. 5.1 Chondrite-normalized REE patterns for the Diorite rock of Dutsen Danbakoshi after Boynton (1984)

5.5 GEOCHEMISTRY OF THE QUARTZ-TOURMALINE ROCK

5.5.1 Major element distribution

The major element geochemical data obtained on the Quartz-tourmaline samples from Dutsen Danbakoshi area are presented in Table 1. The Quartz-tourmaline rock SiO_2 content range from (57.97 – 35.41wt %) with average (46.396wt %). The Alkali oxide content of the Quartz-tourmaline is low Na_2O having an average (0.6262 wt %), K_2O averages (0.092 wt %) and CaO with average (1.574 wt %), low MgO averages (2.542 wt %) and high Fe_2O_3 (T) with average (21.412 wt %)

5.4.2 Trace elements distribution

The geochemical data of the Quartz-tourmaline samples from the study area show variation of the trace elements concentration as in Table 2 The Quartz-tourmaline rocks are enriched in V (0.095 – 242 ppm), Cr (0.018 – 180 ppm), Ni (0.057 – 120 ppm), Sr (0.59 – 1200 ppm), W (0.23 – 300 ppm), Zr (0.38 – 281 ppm) and depleted in Ba (0.04 – 254 ppm) when compared to the average crustal composition of 456 ppm Rudnick and Gao (2003)., Rb (0.5 – 10 ppm) when compared to the average crustal composition of 49 ppm Rudnick and Gao (2003).

The REE abundances was normalized after Boynton (1984) and plotted in Fig. 5.2. The REE fractionation pattern is characterized by enrichment in (LREE) and depletion in (HREE) with negative Eu anomaly and negative Ce anomaly.

Table 7 Chondrite-normalized REE values of quartz-tourmaline

Sample No	TmN	YbN	LuN	Eu/Eu*	LaN/ YbN	LaN/ SmN	CeN/ YbN	CeN/ SmN	EuN/ YbN	Sum REE
MK06	10	9.09	8.24	0.99	4	2.31	2.73	1.58	1.36	66.9
MK07	6	5	4.41	0.84	18.67	4.86	6.03	1.57	2.13	99.35

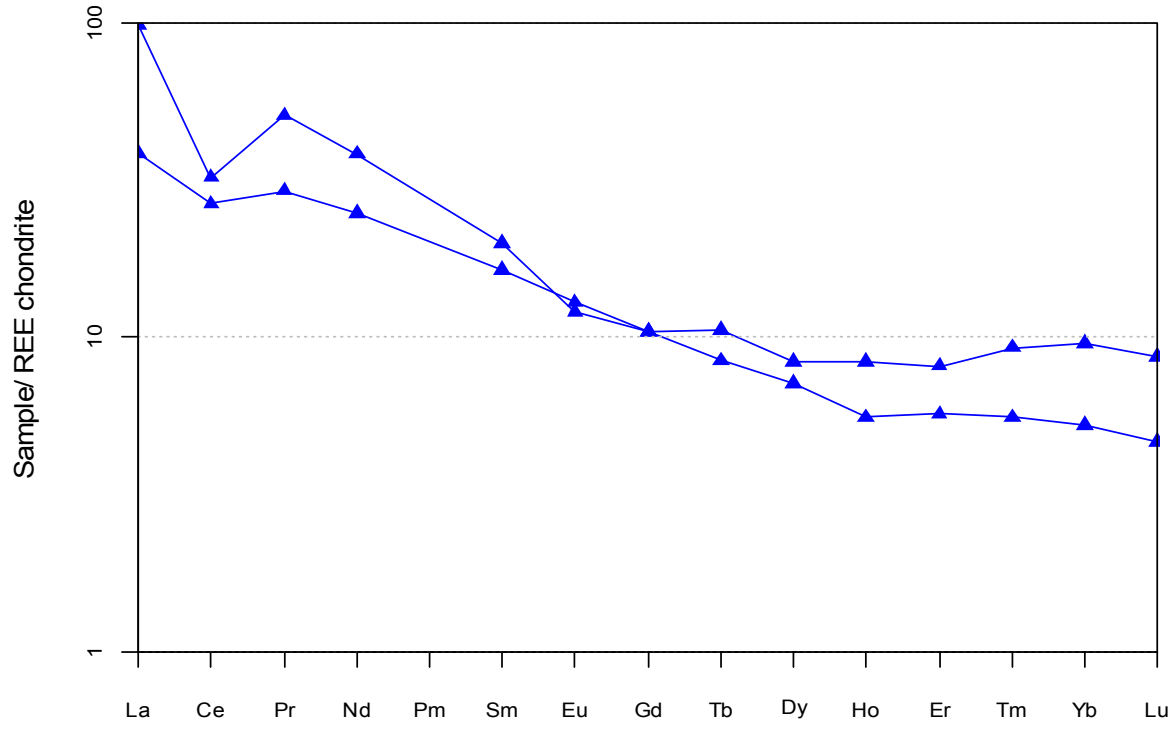


Fig. 5.2 Chondrite-normalized REE patterns for the Quartz-tourmaline rocks of Dutsen Danbakoshi after Boynton (1984)

5.5.3 Boron isotope

The boron isotope values from Dutsen Danbakoshi ranges from – 15.84‰ to – 17.92‰ Table 4

5.6 DISCUSSIONS

A tectonic classification diagram Fig 5.3 shows that the granites are syncollisional in nature; this is in line with Batchelor and Bowden (1985). The silica saturated granites were therefore probably formed through syncollisional processes related to subduction magmatism

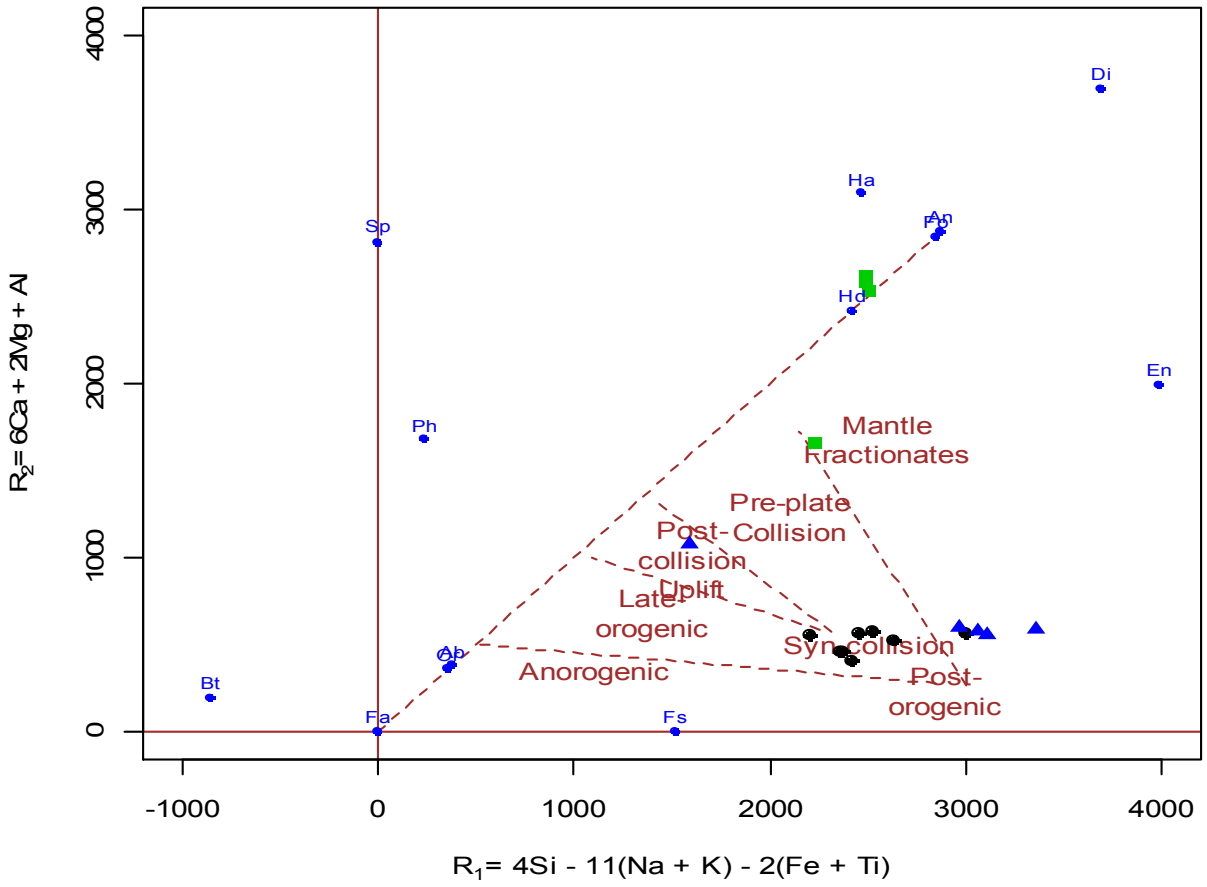


Fig. 5.3 Discriminant diagram for the granite after (Batchelor and Bowden (1985).

Trace elements content from both the host rocks (granites and diorite) and quartz-tourmaline has shown enrichment in light rare earth elements (LREE) and depletion in heavy rare earth elements (HREE) with negative Eu anomaly. The enrichment in (LREE) is signifying immobility of LREE such as La, Ce, Pr,Nd in relative to HREE like Gd, Tb, Dy,Lu and indicating continental or crustal source due to depletion in LREE in the mantle as a result of partial melting over the course of geologic time.

The negative Eu anomaly in the (REE) patterns of silicic rocks are often interpreted to be an indication that a rock has evolved by means of differentiation. Kolionen and Rosenberg (1974), McCathy and Kable (1978) have shown that very similar Eu-depleted distributions may be expected of granites derived from matasedimentary rocks by anatexis. The negative Eu anomaly is probably indicating the formation of both the host rocks (granite and diorite) and quartz-tourmaline in an Upper Proterozoic metasedimentary environment Garba (2003a), Mohamed and Hassanen (1997). The quartz-tourmaline has negative Cerium (Ce) anomaly indicating its formation under oxidizing conditions Garba (2003b).

The host rocks and the quartz-tourmaline have similarities in geochemical signatures that are enrichment in light rare earth element (LREE) and depletion of heavy rare earth element (HREE) with negative Eu anomaly, indicating that the fluid that lead to the tourmalinization might have originated from the host rocks during the hydrothermal process.

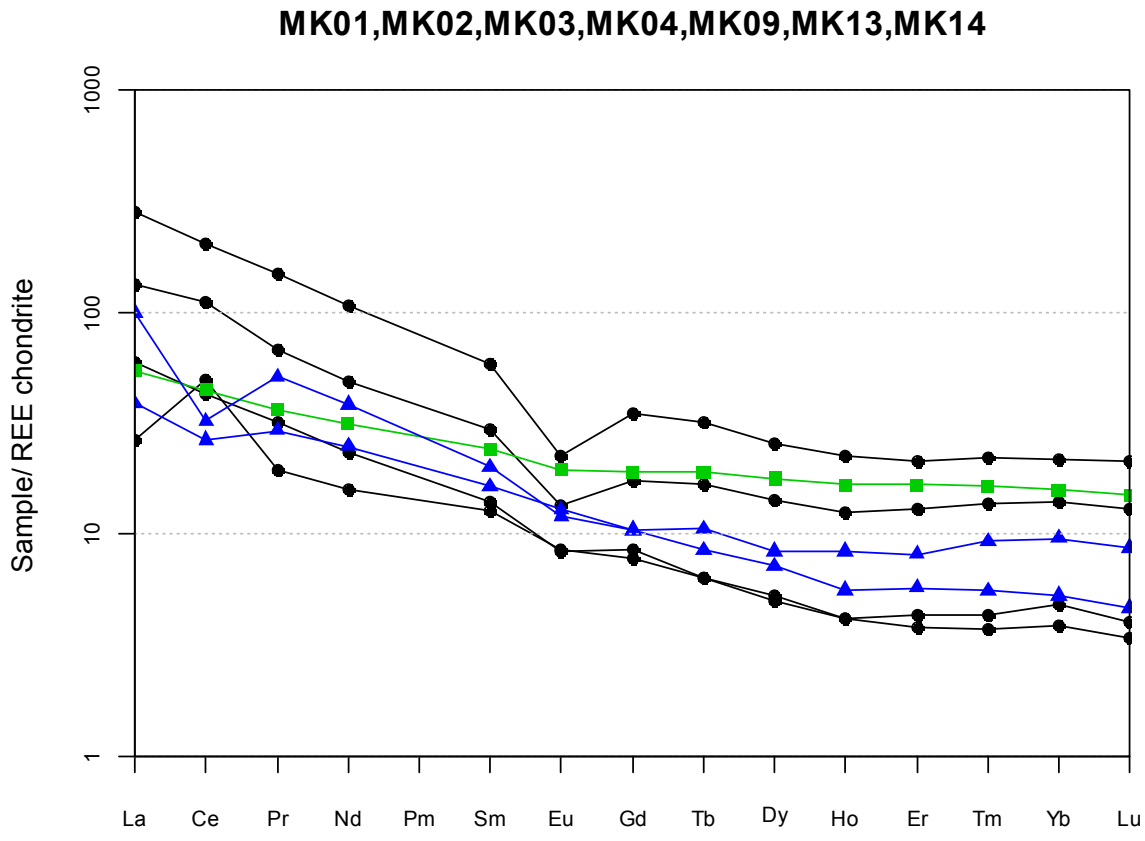


Fig. 5.4 Chondrite-normalized REE patterns for the rocks of Dutsen Danbakoshi area with granite = black, diorite = green and quartz tourmaline = blue, after Boynton (1984)

In minerals and fluids Boron is generally bonded to oxygen as tetrahedral or triangular oxysalt complexes. B only occurs in one oxidation state in natural materials, and B isotopic fractionation is generally controlled by the partitioning of B isotope between the tetrahedral and triangular species, where ^{11}B favours the triangular coordination and ^{10}B favours tetrahedral coordination Palmer and Swihart (1996), Kotaka (1973), Kakihana et al., (1977). In recent years chemical and B isotopic composition of tourmaline have been used as a geochemical tracer in studies of ore

genesis and petrogenesis Palmer and Swihart (1996), Slack (1996), Jiang et al., (1997, 2000), Jiang (1998).

Previous studies on B isotope show that B isotopes can vary in natural sample and reservoir by as much as 80% Barth (1993), Palmer and Swihart (1996). As a highly mobile element during magmatic and fluid related processes, B is preferentially enriched in late exsolved volatile rich fluid, and the exsolution of these fluids leads to depletion of B and other fluid mobile elements in granites Dingwell et al., (1996), London et al., (2002). In most cases, tourmaline is the only significant B sink in granite hydrothermal systems.

Tourmaline is only stable at low pH (Morgan and London, 1989), so triangular coordinated B is the only stable B species in solution in equilibrium with tourmaline. Therefore, tourmalines should be enriched in ^{11}B and have high $\sigma\,^{11}B$. However, tourmalines can have low $\sigma\,^{11}B$ values e.g Palmer and Slack (1989). Based on the results of adsorption experiments on clay Palmer et al., (1987) proposed that incorporation of B in aluminosilicates proceeds initially by adsorption of trigonal $B(OH)_3$ onto mineral surfaces. The coordination of the B atom changes from triangular in solution to tetrahedral in the adsorbed species where the adsorbed species is enriched in ^{11}B. Therefore, the transition from triangular to tetrahedral controls the isotope fractionation, and suggests that B is incorporated into the structure of the mineral without further isotope fractionation allowing very low $\sigma\,^{11}B$.

Tourmalines occur in a variety of geological environments Leeman and Sisson (1996) and most tourmaline have $\sigma\,^{11}B$ values - 30‰ to + 20‰ Fig 5.5 The majority of tourmalines hosted in granite – pegmatite systems have $\sigma\,^{11}B$ values that range from - 10‰ to + 10‰ Fig 5.5 which is characteristic of granitic source for B. However, not all tourmaline bearing granitic rocks are the

result of B rich magmas and tourmaline may be post magmatic in origin (Dingwell et al., 1996) and reflect isotopically higher or lower $\sigma^{11}B$ values.

Extremely low $\sigma^{11}B$ values for tourmaline have been reported at Broken hill, Australia (- 27‰ to - 23‰) Palmer and Slack (1989) and the Lavicky leucogranite. Czech Republic (- 37.3‰ to - 21.3‰) Jiang et al., (2003). As non-marine evaporates are the only known B reservoirs with $\sigma^{11}B$ values less than - 20‰ Swihart et al., (1986).

The quartz bearing tourmaline in this study area is derived from granite and diorite with $\sigma^{11}B$ values that range from – 15.84‰ to – 17.92‰ signifying continental or crustal origin of the boron enriched residual fluids which led to the tourmalinization and also indicating possible dual provenance of B from high pressure metamorphic rocks or granite and pegmatite as in Fig 5.5 which is similar to those in granite related Sn deposits, in South China with $\sigma^{11}B$ values from - 10‰ to - 18‰ Jiang et al. (2003) and is different from $\sigma^{11}B$ values of Cu bearing gem tourmaline in Nigeria which range from – 30.5‰ to - 25.7‰ Shabaga et al., (2010).

The B isotope values in this study are low and generally reflecting the lower end of continental or crustal source as in Fig. 5.5. When compared to $\sigma^{11}B$ values in Cu bearing gem tourmaline in Nigeria, the values are lower than this study which is indicating non marine evaporatic source Shabaga et al., (2010). These differences in $\sigma^{11}B$ values between the Cu bearing gem tourmaline and this study suggest that at least there are different degrees of crustal assimilation or possibly more than one source of B during the crystallization process, which led to higher $\sigma^{11}B$ values in this study than in Cu bearing gem tourmaline for which non marine evaporate source seem to be the dominant source of B.

Although several studies have shown large variations in tourmaline from granite and pegmatite (~30‰) tourmalines from an individual magmatic body generally have a narrow range in $\sigma^{11}B$ values (< 5‰) Swihart and Moore (1989) Chaussidon and Albarede (1992), Smith and Yardley (1996), Jiang and Palmer (1998), Tonarini et al. (1998). This study show that Dutsen Danbakoshi tourmalines have a range in $\sigma^{11}B$ values (1.65‰) that is typical of tourmaline from a single magmatic source.

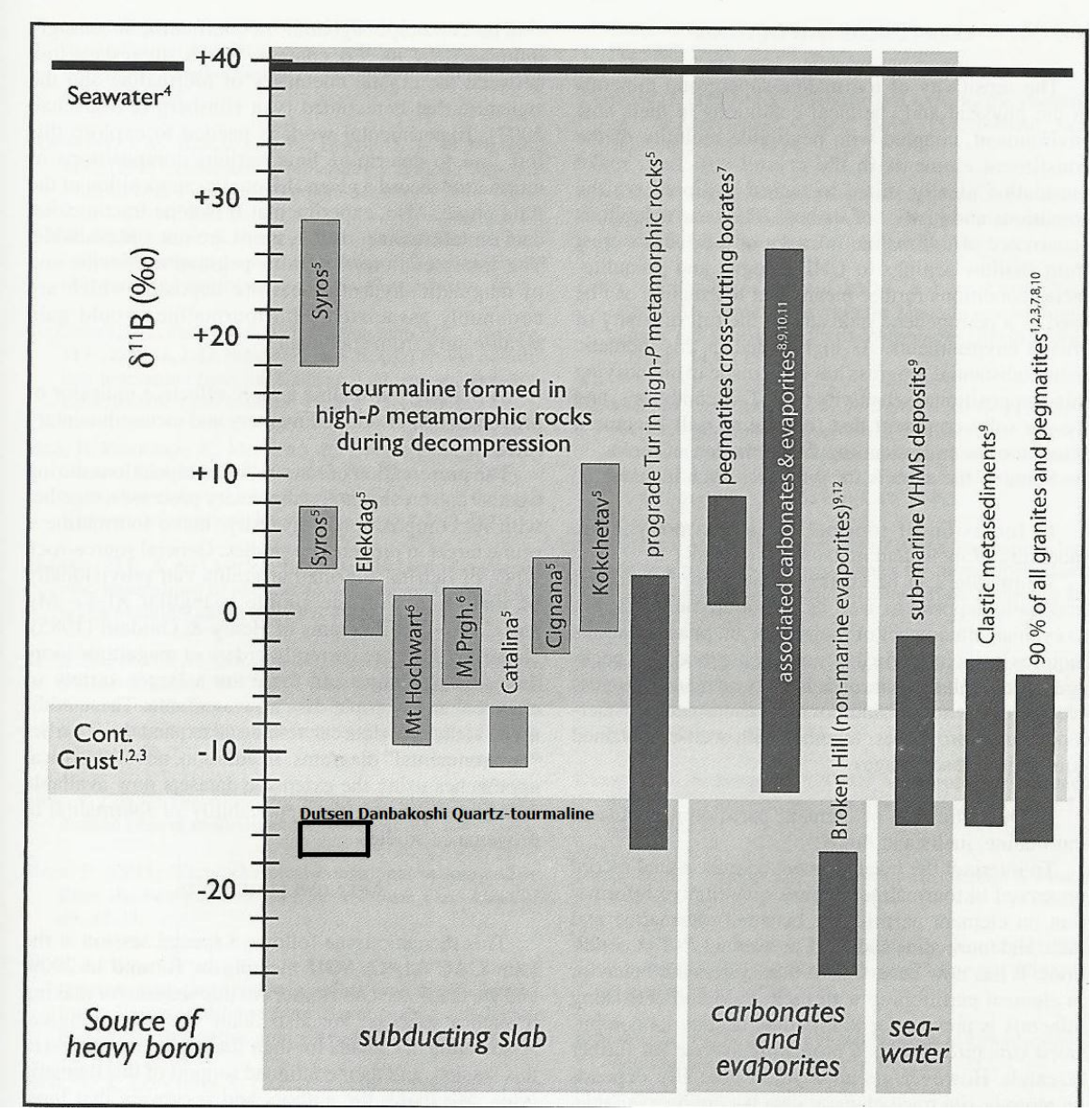


Fig. 5.5 Compilation of boron isotope data of tourmaline from different host-rock and various inferred sources of boron, after Chaussidon & Albarede (1992), Kasemann et al., (2000), Marschall & Ludwig (2006), Foster et al., (2010), Marschall et al., (2009a), Marocchi et al., (2011), Jiang & Palmer (1998), Swihart & Moore (1989), Palmer & Slack (1989), Trumbull et al., (2011), Klemme et al., (2011), Xavier et al., (2008)

5.7 Model of Origin

Underlying the Dutsen Danbakoshi area are rocks of the Nigerian basement complex which are product of a series of Orogenic events McCurry (1976). The rocks mapped include Granite, Metasandstone, Diorite, and Quartz-tourmaline.

Age determination from different parts of the basement complex shows that it has witnessed at least three Orogenic events from Achaean to Pan African. Hence, it's poly–cyclic in nature. The Pan African Orogeny resulted in the emplacement of the Granitoids in the basement complex. Evidences from the present study show that the quartz-tourmaline fluid in this study is derived from the Granitoids as residual fluids following the magmatic differentiation that led to the formation of different granitic rocks such as granites and diorites found in this area. The $\sigma^{11}B$ values ranges from – 15.84‰ to – 17.92‰ signifying continental or crustal origin of B enrich residual fluids which led to the tourmalinization. This therefore indicates that the material for the formation of the granitoids in this study might have been sourced from the partial melting of crustal rocks. However the B isotope values also indicate that the quartz-tourmaline rocks might have dual provenance as in Fig 5.5. From this figure it can be argued that part of the Quartz-tourmaline fluids were generated from high pressure metamorphic rocks. The REE distribution pattern of both the host rocks and quartz-tourmaline has shown enrichment in LREE and depletion of HREE indicating syngenetic relationship. The rocks from the study area are deformed, jointed or sheared in N-S or E-W direction and therefore serves as channel ways that allow B enrich residual fluids that are highly mobile and under tremendous pressure to come to the surface after the consolidation of the silicate rocks, which led to the deposition of Quartz-tourmaline rocks within the area

CHAPTER 6

CONCLUSION AND RECOMMENDATION

6.1 Conclusion

Evidences from field mapping and petrographic studies show that the mapped area is underlain by rocks of basement complex; the evolution of the rocks has been linked to at least three past tectonic events ranging from Achaean to Pan African events

Structural elements in Dutsen Danbakoshi area such as joints, shears exhibit either N-S or E-W trends, these trends are consistent with the stress direction of the Pan African Orogeny. Therefore in the mapped area four rock types were distinguished as follows, the Diorite, the Granite, the Quartz-tourmaline and Metasandstone respectively.

Petrographic studies have confirms that the granites are made up of quartz, microcline and biotite as major minerals; the Diorite is composed of plagioclase, hornblende, quartz and biotite. The Metasandstone consists mainly of quartz and feldspar. The quartz-tourmaline is principally composed of tourmaline and quartz.

The rocks in the study area have shown enrichment in the light rare earth elements (LREE) and depletion in the heavy rare earth elements (HREE) is interpreted as continental or crustal origin due to depletion of LREE due the partial melting of the mantle over the course of geologic time, and negative Eu anomaly is probably indicating the formation of both the host rocks (granite and diorite) and quartz-tourmaline in Upper Proterozoic metasedimentary environment. The negative Ce anomaly is indicating formation of Quartz-tourmaline under oxidizing condition.

The boron isotope values ($\sigma\ ^{11}B$) from Dutsen Danbakoshi quartz-tourmaline are indicating continental or crustal origin of the boron enrich residual fluids which led to the tourmalinization and also indicating possible dual provenance of tourmaline from high pressure metamorphic rocks or granite and pegmatite.

The boron isotope values are also signifying that the granitoids from which the B enrich residual fluids were generated were from the reworking of preexisting basement complex rock. It can also be derived from the B isotope values that the shear zones were the quartz tourmalines are found is also continental or crustal in origin.

6.2 Recommendation

More work is required in order to have in-depth knowledge about Dutsen Danbakoshi tourmaline rich rocks which include:

(1) Fluid inclusion in order to know the temperature at which the tourmalinization fluid forms

(2) More isotopic work is needed to determine age of the tourmaline rich rocks

(3) Electron microprobe is required to know the elemental composition of the Dutsen Danbakoshi quartz-tourmaline rocks.

REFERENCE

Adekoya , J.A. (1996). The Geology and Geochemistry of Maru Banded iron formation north western Nigeria, Journal of African Earth`s Science, 27 (2) 241 – 257

Ajibade, A.C. (1982). The origin and emplacement of Older Granite of Nigeria, some evidence from Zurugeru region. Journal of Mining and Geology Vol. 19 No. 1 221-223

Ajibade, A.C., Woakes, M. and Rahman, M.A. (1987). Proterozoic crustal development in the Pan-African Regime of Nigeria, Copyright of the American Geophysical union.

Ajibade, A.C. and Wright, J.B. (1989). The Togo-Benin-Nigeria shields. Evidence of crustal aggregation in the Pan – African belt. Tectonophysic 165, 125 129.

Bachelor, R.A. and Bowden, P. (1985). Petrologic interpretation of granitoid rocks series using multicationic parameters. Chemical Geology 48, 43-55.

Bacik, P., Meres, S. and Uher, P. (2011). Vanadium rich tourmaline in the metacherts from Chvojnica, Slovonia: crystal chemistry and multistage evolution. Canadian. Mineralogist. 49.

Baksheev, I.A. Prokofev, V.Y., Yapaskurt, V.O., Vigasina, M.F., Zorina, L.D. and Solovev, V.N. (2011). Ferric – iron – rich tourmaline from central Iberia dates the main variscan deformation phases. Geology. Acta. 7, 399 – 412.

Ball, E. (1980). An example of consistent brittle deformation over Late Pan African fracture system of the Tuareg and Nigerian shield. Tectonophysics, 61 (4) 364-379

Barth, S. (1993). Boron isotope variations in nature: a synthesis. Geologische Rundschau, 82, 640 – 65.

Boynton, W.V. (1984). Geochemistry of the rare earth elements: meteorite studies: in Henderson, P., edition,. Rare Earth Element Geochemistry, Elsevier, 63-114

Burke, K.C. and Dewey, J.F. (1972). Orogeny in Africa: in Dessauvagie, T.F.J. and Whitemann, A.J. eds., African Geology, University of Ibadan 1970, 583 – 608.

Chaussidon, M. and Albarede. F. (1992). Secular isotope variations in the continental crust an

ion microprobe study. Earth planet Science letter. 108, 229 – 241.

Dada, S.S. (1998). Crust – forming ages and Proterozoic crustal evolution in Nigeria: A re appraisal of current interpretations Precambrian Research, 87 65

Deksissa, D.J. and Koeberl, C. (2002). Geochemistry and petrography of gold – quartz – tourmaline veins of the Okote area, southern Ethiopia: implications for Gold exploration. Mineralogy and Petrology. 75. 101 – 122.

Dingwell, D.B., Pichavant, M. and Holtz, F. (1996). Experimental studies of boron in granitic melts. in: Boron: Mineralogy Petrology and Geochemistry (E.S. Grew and L.M. Anovitiz editors) Reviews in Mineralogy, 33, Mineralogical Society of America, Chantilly Virginia, U.S.A. . 331 – 379

Dommanget, A., Milesi, J.P. and Diallo, M. (1993). The Loulo Gold and tourmaline-bearing deposit. Mineral. Deposita. 28, 253 – 263.

Ekwueme, B.N. (1995a). Petrogenesis of Schist in Southeast Lokoja, Central Nigeria. Dec-ford, Journal of Pure and Applied. Science. Vol 1. . 70 – 83.

Ekwueme, B.N., and Attoh, K. (1997). Greenstone belts of the West African shield. In: Tectonic evolution of Greenstone belts. (M.J. De wit and L.D Ashwal (Eds)), Oxford Monograph on Geology and Geophysics, Clarendon press, Oxford, 517 – 528.

Elueze, A.A. (2000). Compositional appraisal and petrotectonic significance of the Imelu banded ferruginous rock in the Ilesha schist belt, SW Nigeria. Journal of Mining and Geology, 36 (1) 9 – 18.

Ethier, V.G. and Campbell, F.A. (1977). Tourmaline concentration in Proterozoic sediments of the Southern Cordillera of Canada and their economic significance. Canada Journal of Earth Science 14, 2348-2363

Fargher, M.N. (1961). The Precambrian Geology of the 1:100,000 sheet 52 (ANKA), Sokoto Province. Geology Survey Nigeria (G.S.N) Unpublish Report No. 1324.

Fitches W.R., Ajibade, A.C., Egbunniwe, I.G., Holt. R.W. and Wright, J.B. (1985). Late Proterozoic schist belts and Plutonism in N.W Nigeria. Journal.of Geological. Society. London. 142,319,337.

Foster, G.L., Pogge Von strandmann P.A.E and Rae, J.W.B. (2010). Boron and magnesium isotopic composition of sea water. Geochem. Geophys. Geosys. 11, Q08015.

Gallagher, V. (1988). Coupled substitutions in schorl-dravite tourmaline: New evidence from S.E. Ireland Minerological Magazine 52, 637-650.

Garba, I. (1996). Tourmalinization related to Late Proterozoic – Early Poleozoic lode gold mineralization in the Bin Yauri area, Nigeria. Mineralium Deposita 31, 201- 209.

Garba, I. (2003a). Geochemical discrimination of newly discovered rare metal bearing and barren Pegmatite's in the Pan African (600 + 150 Ma) basement of Northern Nigeria. Transaction of Institution of Mining and Metallurgy. 112. B187 – B292.

Garba, I (2003b). Geochemical characteristics of mesothermal gold mineralization in the Pan Africa (600 + 150 Ma) basement of Nigeria. Transaction of Institution of Mining and Metallurgy. 112. B319 – B325.

Grant, N.K. (1969). The Late Precambrian to Early Paleozoic Pan–African Orogeny in Ghana, Togo, Dahomey and Nigeria. Geological. Society of America Bulliten, 80, 45 – 56.

Grant, N.K. Hikam, M. Burkholder, F.R. and Powell J.L.(1972). Kibaran metamorphic belt in Pan African domain of West Arica. Nature of physical science. 38 (1 1-12

Grant, N.K. (1978). Structural distinction between a metasedimentary cover and an underlying basement in the 600 Ma Old Pan African domain of north western Nigeria. Geological Society of America. Bulletin 89,45-46

Henry, D.J. and Guidotti, C.V (1985) Tourmaline as a petrogenetic indicator mineral, an example from the staurolite – grade metapelites of NW Maine. American Mineralogist, 70, 1 – 15.

Henry, D.J. and Dutrow, B.L. (1992). Tourmaline in low grade classic metasedimentary rock; an example of the petrogenetic potential of tourmaline. Contributions of Mineralogy to Petrology. 112, 203-218.

Henry, D.J. and Dutrow, B.L. (1996). Metamorphic tourmaline and its petrologic applications. In: Boron: Mineralogy, Petrology and Geochemistry (E.S. Grew and L.M. Anovatiz editions) Review of mineralogy. 33. 503 – 557.

Henry, D.J. and Dutrow, B.L. (2001). Compositional zoning and element partitioning in Nickeloan tourmaline from Metamorphosed karst bauxite from Samos, Greece. American. mineralogist. 80, 1130 – 1142.

Hezel, D.C., Kalt, A., Marschall, H.R., Ludwig, T. and Meyer, H.P. (2011). Major element and Li, Be compositional evolution of tourmaline in an S-type granite-pegmatite system and its country rocks,. an example from the island of Ikaria, Aegean Sea, Greece. Canadian. Mineralogist. 49.

Holt, R., Egbuniwe, I.G., Fitches W.R. and Wright J.B. (1978). The relationship between low grade metasedimentary belts, calc-alkaline volcanism and Pan-Africa Orogeny in NW Nigeria. Geol Rundsch, 67, 631 – 646.

Hubbard, F.H. (1975). Precambrian crustal development in western Nigeria: indications from the Iwo region. Bulletin Society of America, 86, 548-554.

Jiang, S.Y. Palmer, M.R., Peng, Q.M. and Yang, J.H. (1997). Chemical and stable isotopic composition of Proterozoic metamorphosed evaporates and associated tourmalines from the Houxlanyu borate deposit, eastern Liaoning, China Chemical Geology, 135, 189 – 211.

Jiang S.Y. and Palmer, M.R. (1998). Boron isotopic systematic of tourmaline from granites and Pegmatites: A synthesis European Journal of Mineralogy, 10, 1253 – 1265.

Jiang, S.Y. (1998). Stable and radiogenic isotope studies of tourmaline: An overview. Journal of. Czech. Geological. Society. 43, 75 – 90

Jiang, S.Y., Palmer, M.R., Slack, J.F. and Anderson, D. (2000). Chemical and boron isotopic

compositions of tourmaline from massive sulphide deposits and tourmalinites in the Mesoproterozoic Belt and Purcell supergroups, Southeastern British Columbia and Northwestern Montana. In : The Geochemical Environment of the Sullivan Pb-Zn-Ag Deposit, British Columbia (J.W. Lydon, T. Hoy, J.F. Slack and M.E. Knapp, editors). Special Publications, 1, Geological Association of Canada Mineral Deposits Division, St John's Canada, 336-354.

Jiang, S.Y., Yang, J.H., Novak, M. and Selway, J. (2003). Chemical and boron isotopic compositions of tourmaline from the Lavicky leucogranite, Czech Republic. Geochemical Journal, 37, 545, 556.

Kakihana, H., Kotaka, M., Shohei, S., Nomura M. and Okamoto, N. (1977). Fundamental studies on the ion exchange separation of boron isotopes. Bulletin of the Chemical Society of Japan, 50, 158-163.

Kasemann, S., Erzinger, J. and Franz, G. (2000). Boron cycling in the continental crust of the central Andes from the Paleozoic to Mesozoic, NW Argentina. Contribution to. Mineralogy.and Petrology 140, 328 - 342.

Keller, P., Roda, R.E., Pesquera P.A. and Fontan F. (1999). Chemistry, Paragenesis and significance of tourmaline in pegmatites of the Southern Tin Belt central Namibia. Chem. Geol. 158, 203 – 225.

Klemme, S., Marschall H.R., Jacob, D.E., Prowatke, S. and Ludwig, T. (2011). Trace element partitioning and boron isotope fractionation between white mica and tourmaline. Canadian. Mineralogy. 49, 165 – 176.

Kennedy, W.G. (1964). The structural differentiation of African in the Pan – African (+ 500Ma) tectonic episode. Res. Inst. Africa Geol., Leeds 8th Ann. Rpt Sci. Results 48.

Kolionen T. and Rosenberg R. J. (1974). Rare earth elements in granitic rocks. Lithos 7, 249-

261

Kotaka, M. (1973). Chromatographic separation of boron and nitrogen isotope using pure water as eluent. Ph.D. thesis, Tokyo institute of technology, 163 .

Kusnir, I. (1999) Gold in Mali. Acta Montan. Slovaca 4, 311 – 318

Leeman, W.P. and Sisson, V.B. (1996). Geochemistry of boron and its implication for crustal and mantle processes in: Boron: Mineralogy, Petrology and Geochemistry (E.S Grew and L.M. Anovitz, editors) Reviews in Mineralogy 33, Mineralogical society of America Chantilly, Virginia, U.S.A. . 645 – 708

London, D., Morgan, G.B. and Wolf, M.B. (2002). Boron in granitic rocks and their contact aureoles. in: Boron: Mineralogy, Petrology and Geochemistry (E.S. Grew and L.M. Anovitz, editors). Reviews in Mineralogy, 33, Mineralogical society of America, Chantilly Virginia U.S.A 299 – 330

London, D. (2011). Experimental Synthesis and stability of tourmaline: a historical perspective. Canadian mineralogist. 49. (117 – 136).

Manning, D.A.C. (1982). Chemical and morphological variation in tourmalines from the Hub Kapang batholith of peninsular Thailand, Mineralogical Magazine 45, 139-147.

Marocchi, M., Marschall, H.R., Konzett, J. Tropper, P., Ludwig, T., Mair, V. and Bargossi, G.M. (2011). Metasomatic, tourmaline in hybrid contact – bands between gneiss and peridotite in the Ulten zone of the Eastern Italian Alps. Chemistry and boron isotopic composition. Canadian. Mineralogist. 49, 245 – 261.

Marschall, H.R. and Ludwig, T. (2006). Re-examination of the boron isotopic compositions of tourmaline from the Lavicky granite, Czech Republic by secondary ion mass spectrometry back to normal. Journal of Geochemistry.40, 631 – 638.

Marschall, H.R., Korsakov, A.V., Luvizotto, G.L., Nasdala, L. and Ludwig, T. (2009a). On the occurrence and boron isotopic composition of tourmaline in (ultra) high –

pressure metamorphic rocks. Journal of Geological society, London. 166, 811 – 823.

Morgan, G.B. London, D. (1989). Experimental reactions of amphobolites with boron bearing aqueous fluids at 200 MPa: implications for tourmaline stability and partial melting in mafic rocks. Contribution to Mineralogy and Petrology 102, 218- 297.

McCarthy T. S. and Kable E. J. D. (1978). On the behavior of rare earth elements during partial melting of granitic rock. Chem. Geol. 22, 21-29

McCurry, P. (1970). The geology of Degree sheet 21 (Zaria), Nigeria, Unpublished M. Sc. Thesis. Ahmadu Bello University, Zaria.

McCurry, P. (1973) Geology of degree sheet 21 (Zaria). Overseas Geol. Min Res., 45, H.M.S.O. London.

McCurry P. (1976). The Geology of the Precambrian to Lower Paleozoic rocks of Northern Nigeria, a review in Geology of Nigeria. 1nd Revised Edition. C.A. Kogbe, , Elizabethan Publication. Lagos . 15 – 39.

McCurry, P. (1978). Geology of Degree sheet 10 (Zuru), 20 (chafe) and part of 9 (Katsina) Nigeria. Overseas Geol. Min. Res., 53 H.M.S.O. London.

McCurry, P. (1989). Geology of the Precambrian to Lower Paleozoic rocks of NW Nigeria: a review: (ed) Geology of Nigeria 2nd Revised Edition C.A. Kogbe. Elizabethan Pubication. Lagos Nigeria 15 – 39.

Michialids, K.M. (1998). Tourmaline concentration in metasedimentary rocks of the Efkarpia Gerakario area in Macedonia, Northern Greece. Chemie. Erde. 58, 80-97.

Mohamed, F.H. and Hassanen, M.A. (1997). Geochemistry and petrogenesis of Sikait Leucogranite Egypt: an example of S-type granite in a metapelitic sequence. Geologic Rundsch. 86, 81 – 92.

Morgan, G.B. and London, D. (1989). Experimental reactions of amphibolites with boron bearing aqueous Fluids at 200 Mpa: Implications of tourmaline stability and partial

melting in mafic rocks. Contributions to Mineralogy and Petrology, 102, 281 – 297.

Nascimento, M.S., Goes, A.M., Macambira M.J.B. and Brod, J.A. (2007). Provenance of Albian sandstones in the Sao Luis – Grajau Basin (Northern Brazil) from evidence of Pb – Pb zircon ages, mineral chemistry of tourmaline and paleocurrent data. sed. Geol. 201, 21 – 42.

Nicoloson, P.M. (1980). The geology and economic significance of the golden dyke dome Northern Territory. In; Ferguson, J., Globy, A.B. (Eds), Uranium in the pine creek geosyncline. International Atomic Energy Agency, Vienna, Austria, 319-334.

Ogezi, A.E.O. (1977). Geochemistry, and Geochrolonogy of Basement Rocks. From North western Nigeria. Unpublished P..h.D. Thesis University of Leeds, England.

Palmer, M.R. Spivack, A.J. and Edmond J.M. (1987). Temperature and PH controls over isotope fractionation during adsorption of boron on marine clay. Geochemica et Cosmochimica Acta, 51 2319 – 2323.

Palmer, M.R. and Slack J.F. (1989). Boron isotope geochemistry: An overview in: Boron: Mineralogy, Petrology and Geochemistry (E.S Grew and L.M. Anovitz, editors). Reviews in Mineralogy, 33, Mineralogical Society of America, Chantilly Virginia, U.S.A.709 – 744

Palmer, M.R, and Swihart, G.H. (1996). Boron Isotope geochemistry: An overview in: Boron: mineralogy, Petrology and geochemistry (E.S. Grew and L.M. Anovitz editors). Review in Mineralogical Society of America, Chantilly, U.S.A. 709 –744.

Rudnick R.L. and Gao S. (2003) Composition of the continental crust. Elsevier 3, 1-64.

Selway, J.B., Cerny, P. and Hawthorne, F.C. (2000). The Tanco pegmatite at Bernic Lake Manitoba. XIV. Internal tourmaline. Canadian Mineralogist. 38, 877-891.

Selway, J.B., Novak, M., Cerny, P. and Hawthorne, F.(1999). Compositional evolution of tourmaline in lepidolite – subtype pegmatites. European. Journal of mineralogy II, 569 – 584.

Shabaga, B.M, Fayek, M. and Hawthorne, F.C. (2010). Boron and lithium isotopic compositions as provenance indicators of Cu-bearing tourmalines, Mineralogical Magazine , Vol. 74 (2), 241-255.

Slack, J.F., (1982). Tourmaline Appalachian- Caledonian massive sulphide deposits and its exploration significance. Trans. Institute of Mining and Metallurgy 91(B), B81-89.

Slack, J.F. (1996). Tourmaline associations with hydrothermal ore deposits in: Boron: Mineralogy, petrology and geochemistry (E.S. Grew and L.M. Anovitz, editors). Reviews in mineralogy, 33 Mineralogical society of America, Chantilly, Virginia, U.S.A.559 – 643

Slack, J. F.and Coad, P.R. (1989). Multiple hydrothermal and metamorphic events in the kidd creek volcanogenic massive sulphide deposit, Timmins, Ontario; evidence from tourmalines and chlorite. Canadian Journal of Earth Sciences 26, 694-715.

Slack, J.F., Herriman, N., Barnes, R.G.and Pilmer, I. R. (1984). Stratiform tourmalinite in metamorphic terranes and their geologic significance, Geology. 12, 713-716.

Slack, J..F. Passchie, C.W. and Zhang, J.S. (1996). Metasomatic tourmalinite formation along basement-cover decollements, Orobic Alps, Italy. Schweizerische Mineralogische Petrographische Mitteilungen 76, 193-207.

Smith, M.P. and Yardley, B.W.D (1996). The boron isotopic composition of tourmaline as a guide to fluid processes in southwestern England orefield. Anion microprobe study. Geochemica et Coschimica Acta, 60, 1415 – 1427.

Swihart, G.H,. Moores P.B. and Callis E.L. (1986). Boron isotopic compositions of marine and non-marine evaporate borates. Geochimica et Cosmochimica Acta, 50, 1297 – 1301

Swihart, G.H. and Moore, P.B. (1989). A reconnaissance of the boron isotopic composition of tourmaline. Geochim. Cosmochim. Acta 53, 911 – 916.

Taylor, S.R. (1965). The application of trace element data to problems of petrology. In L. Ahrens, F. Press, S.k. Runcorn and C. Urey (editions), Physics and Chemistry of the Earth, vol. 6, Pergamon Press, Oxford, 133-214

Tonarini, S., Dini, A., Pezzotta, F. and Leeman, W.P. (1998). Boron isotopic composition of zoned (schorl – elabite) tourmalines, Mt. Capanna Li – Cs pegmatites, Elba (Italy). European Journal of Mineralogy, 10, 941 – 952.

Turner, D.C (1983). Upper Paleozoic schist belts in the Nigeria sector of the Pan – African Province of the West African Precambrian Research. 21, 55 – 75.

Trumbull, R.B., Slack, J.F., Krienitz, M.S., Belkin, H.E. and Wiedenbeck. M. (2011). Fluid sources and metallogenesis in the Blackbird Co-Cu-Au-Bi-Y-REE district. Idaho, U.S.A. Insight from major-element and boron isotopic compositions of tourmaline Canadian Mineralogist 49, 225 – 244.

Van Hinsberg, V.J. and Schumacher J.C., (2011) Tourmaline as a petrographic indicator mineral in the Haut-Allier metamorphic suite, Massif Central, France. Canadian Mineralogist. 49, 177-194.

Von Georne, G. and Franz, G. (2000) Synthesis of Ca – tourmaline in the system CaO – MgO – $A1_2O_3$ – SiO2 – B_2O_3 – H_2O – Hcl. Mineral. Petrol. 69, 161 – 182.

Von Goerne, G., Franz, G. and Heinrich, W. (2001). Synthesis of tourmaline solid solutions in the system Na_2O - MgO - Al_2O_3 - SiO_2 - B_2O_3 - H_2O - Hcl and the distribution of Na between tourmaline and fluid at 300 to 700^{0}C and 100 Mpa. Contribution to. Mineralogy and Petrol. 141, 160 – 173

Werding, G. Schreyer, W. (1984). Alkali free tourmaline in the system MgO-Al_2O_3-SO_2-B_2O_3-H_2O. Geochemical Cosmochimica Acta. 48, 1331-1344.

Williamson, B.J., Spratt, J., Adams, J.T., Tindle, A.G., and Stanley, C.J. (2000). Geochemical constraints from zoned hydrothermal tourmalines on fluid evolution and Sn mineralization: an example from fault breccias at Roche, SW England. Journal of

Petrology 41, 1439-1453.

Willner, A.P. (1992). Tourmalinites from the stratiform peraluminous metamorphic suites of the Central Namaqua Mobile Belt (South Africa). Mineralium Deposita 27,304-313.

Wright, J.B. (1976). Fracture systems in Nigeria and initiation of fracture zones in the South Atlantic. Tectonophysics, 34, 143-147.

Wright, J.B., and Mc Curry, P. (1970). A reappraisal of some aspects of Precambrian Shield Geology; Discussion, Bulletin of. Geological Society America. 81, 3491 – 3492.

Wright, J.B. Hastings D.A., Jones, W.B. and Williams, H.R (1985). Geology and Mineral Resources of West Africa. Allen and Unwin. London

Xavier, R.P., Wiedenbeck, M., Trumbull, R.B., Deher, A.M., Monteiro L.V.S., Rhede, D., De Araujo, C.E.G.and Torresi, I. (2008). Tourmaline B-isotopes fingerprint marine evaporites as the source of high – salinity ore fluids in iron oxide copper – gold deposits. Carajas mineral province (Brazil). Geology 36, 743 – 746.

APPENDIX 1

Joint readings (in degrees) on the medium grained granite

Joint readings (in degree)	Frequency
46^0	2
48^0	6
50^0	4
51^0	1
52^0	4
54^0	4
56^0	1
61^0	1
146^0	1
148^0	2
149^0	1
156^0	2
158^0	1
160^0	1
166^0	1

APPENDIX 2

Joint readings (in degrees) on the medium grained granite

Joint readings (in degree)	Frequency
20^0	2
22^0	3
23^0	1
24^0	5
25^0	1
26^0	7
28^0	3
29^0	1
30^0	3
150^0	2
152^0	4
156^0	2
158^0	2